Lakehead University

The Phase Behaviour of Isopropanol/Water/NaCl Mixtures at Atmospheric Pressure

by

Saeed Ataee-Ataabadi

Thesis submitted in partial fulfillment of the requirements

for the Master of Science

in

Chemical Engineering

Supervisor

Dr. Francisco Ramos-Pallares

Thunder Bay, Ontario

March 2023

Abstract

Alcohol-based biofuels will play a key role in substituting the fossil fuels used in transportation and power generation. Compared to fossil fuels, alcohol-based biofuels have a lower carbon footprint and can be produced from the fermentation of biomass. Moreover, some branched alcohols have similar properties to those of gasoline which makes them suitable chemicals to produce gasoline-like biofuels. To produce high-purity fuel-grade alcohols, the produced alcohol must be separated from the aqueous fermentation broth usually through distillation. However, distillation is an energy-intensive operation with a high carbon footprint; and the presence of azeotropes of alcohol/water makes distillation very expensive and technically challenging. The addition of some salts to the fermentation broth triggers a liquid-liquid phase splitting. One of the liquid phases is rich in alcohol and the other is rich in water. Therefore, understanding the phase behaviour of alcohol/water/salt mixtures is very important in the design of liquid-liquid operations for alcohol production.

The goal of this study was the experimental investigation of the phase behaviour of the isopropanol/water/sodium chloride (NaCl) mixtures at atmospheric pressure. Isopropanol was chosen as it is a branched alcohol, readily available, and can be salted out from an aqueous solution using NaCl. To achieve this goal, several experimental techniques were developed and validated to collect liquid-liquid, liquid-liquid-solid, liquid-solid, and vapor-liquid equilibrium data at atmospheric pressure. The liquid-liquid, liquid-liquid-solid, and liquid-solid data were collected at temperatures from 0 to 70°C and included liquid-liquid phase boundaries and phase compositions. The vapor-liquid dataset includes saturated liquid and saturated vapor compositions as well as normal boiling point temperatures. The results showed that liquid-solid and liquid-liquid boundaries were not significantly affected by the temperature. Regarding liquid-liquid phase compositions, the isopropanol mass content in the alcohol-rich phase increased from 0 to 50°C and did not change significantly when the temperature was increased from 50 to 70°C. For vapor-liquid equilibrium, the normal boiling point of the isopropanol/water/NaCl mixture decreased and the isopropanol content in the vapor phase increased at higher NaCl content in the liquid. These results indicate that the presence of NaCl increases the relative volatility of isopropanol.

Acknowledgments

I wish to acknowledge the significant contributions and support of several individuals without whom the successful completion of this dissertation would not have been possible.

I would like to express my heartfelt appreciation to my supervisor, Dr. Francisco Ramos-Pallares, for his guidance, expert advice, and unwavering support throughout the research process. His timely feedback, constructive criticism, and mentorship have been critical to the success of this study.

In particular, I am deeply thankful to my family, and most notably, my wife, for her unwavering support, encouragement, and belief in me. Her love, patience, and understanding have been a constant source of motivation, especially during challenging times. Her steadfast support has enabled me to remain focused on my studies and pursue my goals with confidence.

I extend my appreciation to my teammate, Twaha Mohamed, for his invaluable support throughout this research. I would also like to thank Mr. Garry Rathje for generously allowing me to use his lab's equipment for this research.

Finally, I would like to acknowledge the participants who willingly shared their time, knowledge, and experiences, without whom this research would not have been possible. I am grateful for their willingness to take part in this study and for the significant impact their contributions have had on my research findings.

Table of Contents

List of Figures

List of Tables

List of Symbols and Abbreviations

BCHA	Branched-Chain Higher Alcohols
ATPS	Aqueous Two-Phase System
MTPA	Metric Tons Per Annum
RI	Refractive Index
MW	Molecular Weight
NRTL	Non-Random Two-Liquid activity coefficient model
UNIQUAC	Universal Quasichemical activity coefficient model
PRT	Platinum Resistance Thermometer
AARD	Average Absolute Relative Deviation
STL	Slop of Tie-Line
PP	Plait Point

P	Pressure
T	Temperature
O	Organic phase
A	Aqueous phase
R	Universal gas constant (8.314 $kJ.kmol^{-1}.K^{-1}$)
R^2	Correlation coefficient
T_b	Boiling point
T_c	Critical temperature
P_c	Critical pressure
A	Temperature dependent parameter Eq.4.1
B	Temperature dependent parameter Eq.4.1
C	Temperature dependent parameter Eq.4.1
D	Temperature dependent parameter Eq.4.2
E	Temperature dependent parameter Eq.4.2
L	Single-liquid phase
L_1	Water-rich phase
L_2	Isopropanol-rich phase
LL	Two-liquid phase
S	Solid phase
VLE	Vapor-Liquid Equilibrium
VL	Vapor-Liquid phase
LLV	Liquid-Liquid-Vapor phase
SLLV	Solid-Liquid-Liquid-Vapor phase
wt	Mass fraction

wt%	Mass fraction percent
a_I	Activity of isopropanol Eq. 2.11
a_W	Activity of water Eq. 2.12
μ_i	Chemical potential of component *i*
ω	Acentric factor
w	Mass fraction Eq. 3.2
x_i	mole fraction
γ_i	Activity coefficient of component *i*
a_i	Activity of component *i*
v	Number of moles
β	Binary interaction Eq. 3.2
ϕ	Fugacity coefficient

Chapter 1: Introduction

The role of biofuels such as ethanol, biodiesel, and ethanol blends, has rapidly increased in the last 20 years due to the concerns related to carbon emissions produced by transportation. In the United States, in 2020, 27% of the total carbon emissions were produced from the transportation sector, compared to 25% produced from electric power generation, 24% from the industry, 13% from residential and commercial sectors, and 11% from agriculture (EPA Agency, 2020). The higher emissions from the transportation sector compared to those in the other sectors have triggered the development of technologies and processes to increase the production and the quality of produced biofuels. Ethanol is the most widely used alcohol for biofuel production. The worldwide amount of ethanol produced in 2021 was 27 billion barrels with the United States as the largest producer with 15 billion barrels and Canada, one of the small producers, with 0.43 billion barrels (US Department of Energy, 2022). According to the International Energy Agency, the worldwide production of ethanol required to meet the 2050 zero carbon emissions scenario must growth at least 16% per year (International Energy Agency, 2022). However, despite the very important role of ethanol in the production of biofuels, this alcohol is not ideal for biofuel production because:

- It has a lower energy density compared to gasoline (Atsumi *et al.,* 2008).
- It is hygroscopic. The chemical affinity between ethanol and water causes the water in the air to dissolve into the fuel, potentially triggering a liquid-liquid phase separation which reduces the quality of the fuel (Kunwer *et al.,* 2022).
- It is corrosive. Transportation and storage of ethanol may lead to corrosion issues in pipelines and tanks as ethanol reacts with the oxygen in the air producing acidic compounds (Arifin *et al.,* 2014).
- It forms a lower boiling point azeotrope with gasoline. The presence of this azeotrope increases the volatility of the fuel negatively impacting the efficiency of combustion engines (Demenezes *et al.,* 2006; Da Silva *et al.,* 2005(a); Kunwer *et al.,* 2022).

Because of these reasons, higher alcohols with carbon numbers of 3, 4, or 5 are being investigated as potential substitutes for ethanol. Particularly the branched members of these families as they have energy densities closer to gasoline, are not hygroscopic and are less volatile compared to ethanol (Atsumi *et al.,* 2008; Brownstein, 2015). Examples of branched higher alcohols with

potential applications in the production of biofuels and fuel blends are isopropanol, isobutanol, tert-butanol 2-methyl-1-butanol, and 3-methyl-1-butanol. These branched alcohols are known as branched-chain higher alcohols (BCHAs). However, the industrial production of these branched alcohols depends greatly on: 1) the development of biological processes for their production from aqueous fermentation of biomass; and 2) the understanding of the phase behaviour of mixtures containing these alcohols for process design simulation and optimization. This study focuses specifically on the phase behaviour of mixtures of isopropanol and water. Table 1.1 compares the fuel properties of isopropanol and gasoline.

Table 1.1 Selected properties of isopropanol and gasoline. (Sivasubramanian *et al.,* 2017; Andersen *et al.,* 2010; Lebo, 1921; Al-Abdullah *et al.,* 2015; US Department of Energy, 2022). The energy content refers to the lower heating value.

	Isopropanol	Gasoline
Octane Number	105	92
Reid Vapor Pressure, psi	1.79	9
API Gravity	0.78	~ 0.7
Flash Point, ˚C	13	-45
Energy Content x 10^3, (Btu/gal)	86	114

Isopropanol is the simplest member of the BCHA family and is produced either by a catalytic process or by fermentation of biomass. The catalytic process is the most popular industrial way to produce isopropanol and involves the direct or indirect hydration of propylene over a catalyst. The reaction products are isopropanol, water, and some impurities (Y. Xu *et al.,* 2002; Kroschwitz, 1991). The fermentation process involves the biological degradation of biomass by genetically modified bacteria to produce isopropanol as one of the components of the aqueous fermentation broth (Survase *et al.,* 2011; Rochón *et al.,* 2019; Ko *et al.,* 2022). The isopropanol produced by the catalytic or fermentation process needs to be purified before being used as a fuel additive; typically, through azeotropic distillation due to the azeotropic nature of the mixture isopropanol-water (Xu *et al.,* 2002). This azeotropic distillation is usually more expensive and energy-intensive compared to conventional distillation. A potential alternative to separate the isopropanol from the aqueous matrix is liquid-liquid extraction triggered by the additions of salts. The addition of some salts to the aqueous matrix reduces the affinity of the alcohol with the water, facilitating purification. Therefore, mapping the phase behaviour of these electrolyte mixtures is required for designing cost-efficient alcohol-purification operations.

1.1 Knowledge Gaps and Objectives

The fundamental stage in the development of any new technology is the understanding of the thermophysical properties and phase behaviour of the fluids to be used. To study if the addition of salt to an aqueous fermentation broth containing BCHA's has potential applications in the development of new separation technologies, it is then necessary to investigate the effect of the salt on the phase behaviour of the mixture through experimental data collection as it is more accurate than simulation. Experimental data for mixtures containing normal alcohols up to butanol, water and some salts have been reported in the literature; however, there is a scarcity of data on mixtures containing BCHA's, water and salt. Moreover, the data reported for mixtures containing BCHA's is usually not thermodynamically consistent. Thermodynamically inconsistencies indicate the data is not at equilibrium as the equal fugacity criteria is not satisfied despite the other requirements such as the mass balance, equal temperatures and pressures are satisfied. The usage of inconsistent data leads to unreliable calculations and potential fake phase behaviour predictions. Consequently, the motivation for this study is the collection of thermodynamically consistent data on the phase behaviour of mixtures containing BCHA, water, and salt to map the phase diagram of these mixtures.

The main objective of this study is the mapping of the phase behaviour of mixtures containing isopropanol, water, and NaCl; specifically, the solid diagram related to the potential design of separation operations: liquid-solid, liquid-liquid, liquid-liquid-solid, and vapor-liquid. Isopropanol was chosen as it is the simplest member of the BCHA family with potential application as a biofuel additive. Sodium chloride was chosen as the salting-out agent as it is one of the salts widely used in industrial applications due to its availability and low cost. Note, this study is intended to shed light on the thermodynamics of isopropanol/water/NaCl mixtures not to develop a comprehensive study on the design of industrial separation operations.

The specific objectives of this project were to:

1. Develop an experimental methodology to measure the liquid-liquid phase boundary for isopropanol/water/NaCl mixtures at temperatures from room to 70°C at atmospheric pressure.

2. Measure liquid-liquid phase compositions for isopropanol/water/NaCl mixtures at thermodynamic equilibrium at temperatures from 0 to 70°C at atmospheric pressure.
3. Develop a methodology to test the thermodynamic consistency of measured phase compositions.
4. Develop an experimental methodology to measure liquid-vapor equilibrium temperatures and compositions for isopropanol/water/NaCl mixtures.
5. Measure boiling points and liquid-vapor phase compositions for isopropanol/water/NaCl mixtures at atmospheric pressure.

1.2 Thesis Structure

This thesis is divided into five chapters, not including the introduction:

Chapter 2 provides a review of the literature relevant to the phase behaviour of isopropanol/water/NaCl mixtures as well as the state-of-the-art concerning the thermodynamics of these mixtures.

Chapter 3 described the different experimental techniques used in this study for data collection as well as the validation of these techniques.

Chapter 4 focuses on the experimental results and discussion.

Chapter 5 summarizes the conclusions and recommendations for future work.

Chapter 2: Literature Review

This chapter presents a literature review of the experimental and theoretical phase behaviour of alcohol/water/salt mixtures. The first section presents an overview of the chemistry of isopropanol, water, and sodium chloride (NaCl). The second section presents a brief review of the thermodynamics of electrolyte systems containing alcohol, water, and salt as well as the results of the experimental investigation of the phase behaviour of alcohol/water/salt mixtures.

2.1 The Chemistry and thermodynamics of Isopropanol, Water, and Sodium Chloride

2.1.1 Isopropanol

Isopropanol, also known as 2-propanol, propane-2-ol, or isopropyl alcohol, is an organic secondary alcohol with the hydroxyl group attached to an isopropyl alkyl group. The molecular formula of isopropanol is C_3H_8O; and, at room condition, it is a colorless liquid, flammable with an intense odor (Slaughter *et al.,* 2014). Isopropanol is produced from propylene through two different catalytic industrial methods: 1) indirect hydration of refinery-grade propylene; and 2) direct hydration of chemical-grade propylene. Roughly, $3x10^6$ metric tons per annum (MTPA) of isopropanol are produced globally; 30% of this total amount is produced in the US, Europe, and Asia (Panjapakkul *et al.,* 2018). Isopropanol is an important reagent in the pharmaceutical, household, and commercial industries with applications in the production of cosmetics, cleaners, disinfectants, solvents, and different types of antifreeze. In addition, isopropanol has potential applications in the production of biofuels (Atsumi *et al.,* 2008). Isopropanol has similar fuel properties as those of *n*-butanol and iso-butanol and it is the simplest member of the BCHA family used in the preparation of biofuels (Atsumi *et al.,* 2008). In comparison with ethanol, branched-chain alcohols, like isopropanol, are more suitable to produce biofuels because they are less corrosive, and have higher energy and blending capability (Koppolu *et al.,* 2016).

Isopropanol is a polar molecule that self-associate with other isopropanol molecules through hydrogen bonding: the attraction between the negative charge of the oxygen of one molecule and

the positive charge of the hydroxylic hydrogen in another molecule. Due to its polarity and ability to form hydrogen bonding, isopropanol is highly soluble in water at room conditions (Guo *et al.,* 2022). Isopropanol and water form a mixture that is difficult to separate by distillation because of its azeotropic nature. This azeotrope has a lower boiling point of 80.37 °C and a mass composition of 87.7% isopropanol at atmospheric pressure (Hartanto *et al.,* 2019). The molecular structure of isopropanol is shown in Fig. 2.1, and selected thermophysical properties are listed in Table 2.1.

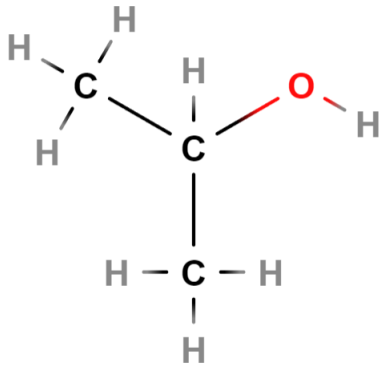

Figure 2.1. Chemical structure of isopropanol. C, H, and O stand for carbon, hydrogen, and oxygen atoms. The solid lines are the covalent bonds.

2.1.2 Water

Water is a transparent and colorless liquid at room conditions with the molecular structure shown in Fig. 2.2. Water is a polar substance and its molecules self-associate through hydrogen bonding interactions. Due to hydrogen bonding, in solution, the molecules of water form big clusters of up to 3 to 50 molecules (Ignatov *et al.,* 2022). The formation of these clusters governs the thermodynamic behaviour of water and is responsible for some of the abnormalities in its thermophysical behaviour, such as higher normal boiling point, higher density, and increasing thermal conductivity with temperature (Ignatov *et al.,* 2022). Some thermophysical properties of water are shown in Table 2.1.

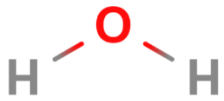

Figure 2.2. Chemical structure of Water. O and H represent oxygen and hydrogen atoms respectively and the solid lines are the covalent bonds.

2.1.3 Sodium Chloride

Sodium chloride (NaCl), usually referred to as salt, is an ionic compound commonly used in the production of dyes, detergents, plastics, pharmaceuticals, and glass (Fuentes-Azcatl and Barbosa, 2016). Sodium chloride is an ionic compound formed by the electrostatic attraction between the sodium (Na^+) cation and the chloride (Cl^-) anion (Fuentes-Azcatl and Barbosa, 2016). At room conditions, sodium chloride is a crystalline solid with solubilities in water and isopropanol of 26.42 and 0.35 wt%, respectively. The solubility of NaCl in water slightly increases with increasing temperature (Pinho and Macedo, 2005). The solubility of NaCl in isopropanol is not significantly affected by the temperature (Kirn and Dunlap, 1931; Larsen and Herschel, 1939). The chemical structure of NaCl is shown in Fig. 2.3, and some of its thermophysical properties are shown in Table 2.1.

Figure 2.3. Chemical structure of sodium chloride. Cl and Na are the chloride and sodium ions respectively.

Table 2.1. Selected physical properties of isopropanol, water, and sodium chloride (NaCl). RI is the refractive index at 25°C; MW is the molecular weight; T_b, T_c, P_c, and ω are the normal boiling point, the critical temperature, the critical pressure, and the acentric factor, respectively. These physical properties were taken from (Sretenskaja *et al.,* 1995; Smith *et al.,* 1965; Muniz *et al.,* 2021; National Institute of Standard and Technology (NIST), 2008).

Components	RI	MW, g/mol	T_b, K	T_c, K	P_c, kPa	Ω	Density, g/ml
Isopropanol	1.3753	60.096	355.45	508.3	4762	0.668	0.79
Water	1.3325	18.015	99.1	647	22100	0.345	0.999
NaCl	-	58.439	-	-	-	-	-

2.2 Thermodynamics of Alcohol/Water/Salt Mixtures

The thermodynamic behaviour of alcohol/water/salt mixtures has been widely studied in the last 30 years as it has potential applications in the design of separation operations to purify alcohols produced from the fermentation of biomass. The final product of the biomass fermentation is an aqueous broth with water content as high as 66 wt% (Torres-Ortegaa, and Rong, 2016, Lin and Tanaka, 2006). The high-water content in the fermentation broth makes the separation of the alcohol by conventional distillation an energy-intensive operation considering the higher heat capacity of the water and the potential presence of azeotropes alcohol-water (Karimi *et al.,* 2021; Cantero *et al.,* 2017). The addition of salt to the fermentation broth reduces the affinity between the alcohol and the water facilitating its separation. For instance, adding salt to the fermentation broth increases the relative volatility of the alcohol which facilitates its separation by distillation (Rongqi and Zhanting, 1999); or adding salt into the broth could trigger a liquid-liquid phase split with one of the liquid phases rich in alcohol and the other phase rich in water (Rongqi and Zhanting, 1999).

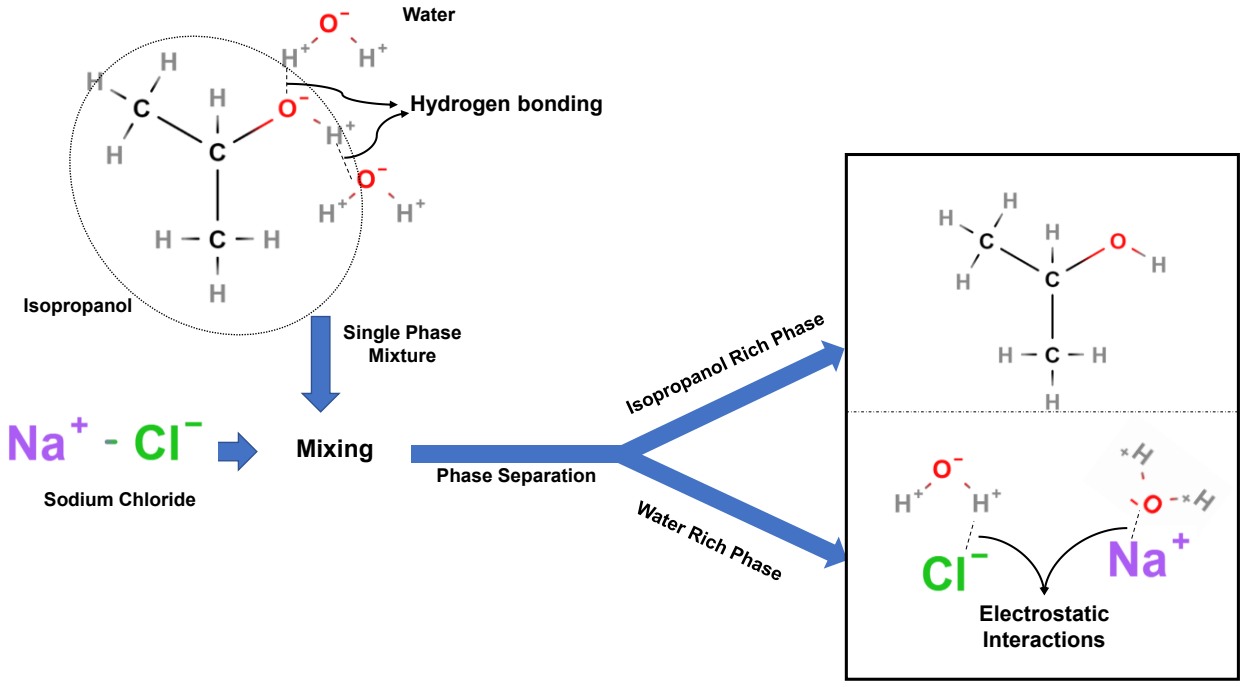

Figure 2.4. Separation of single-phase water/isopropanol mixture after adding sodium chloride into two liquid phases. The top phase is rich in isopropanol (organic or liquid phase) and the bottom phase is rich in water (aqueous or heavy phase).

Fig. 2.4 illustrates the liquid-liquid phase split after adding sodium chloride (NaCl) to a liquid binary isopropanol/water. Isopropanol and water form a single-phase liquid mixture because they are both polar molecules that self and cross-associate through hydrogen bonding. These interactions are responsible for the total miscibility between these two components. However, when NaCl is added to the isopropanol/water binary, the presence of Na^+ and Cl^- ions in the solution disrupts the interactions between isopropanol and water molecules as these ions preferentially interact with the water molecules. This preferential interaction between the ions and the water molecules is due to its higher dielectric constant (78.304) compared to that of isopropanol (19.13) at room temperature (Miller and Maass, 1960; Malmberg and Maryott, 1956). This higher affinity between the ions and water triggers a phase split, *i.e.*, the formation of a second liquid phase composed mainly of the isopropanol molecules displaced out of the original solution as shown in Fig. 2.4 (Briscoe *et al.,* 2000). Therefore, at thermodynamic equilibrium, the system splits into two liquid phases: one rich in alcohol and the other one rich in water. In this study, the alcohol-rich and the water-rich phases will be referred to as the organic and the aqueous phases, respectively.

For engineering applications in the design, simulation, and optimization of separation operations, it is then required the calculation of organic and aqueous phase compositions. This calculation can be performed by using the concepts related to phase equilibrium thermodynamics applied to electrolyte mixtures.

2.2.1 Thermodynamic Modelling

The fundamental concepts of phase equilibrium thermodynamics can be applied to the calculation of the composition of the organic and the aqueous phases. At thermodynamic equilibrium, the following equations must be satisfied (Thomsen, 2009):

$$P^O = P^A \quad (2.1)$$

$$T^O = T^A \quad (2.2)$$

$$\mu_i^O = \mu_i^A \quad (2.3)$$

where P (in kPa) is the pressure, T is the absolute temperature (in K), and μ is the chemical potential (J.mol^{-1}). Superscripts O and A refer to the organic and aqueous phases, respectively.

The subscript *i* refer to any of the components of the system: isopropanol, water, or NaCl. μ is the chemical potential of component i . In an ideal solution, the chemical potential is calculated as follows (Thomsen, 2009):

$$\mu_i^{ideal} = \mu_i^* + RT \ln x_i \tag{2.4}$$

where μ_i^* is the chemical potential of component i in the standard state, which depends on temperature, pressure, and nature of the components; and x_i is the mol fraction of component i. The chemical potential of an electrolyte mixture significantly deviates from that of the ideal solution due to the electrostatic interactions. The excess chemical potential captures this deviation (Thomsen, 2009):

$$\mu_i = \mu_i^{ideal} + \mu_i^{excess} \tag{2.5}$$

The excess chemical potential is given by:

$$\mu_i^{excess} = RTln\gamma_i \tag{2.6}$$

where γ_i is the activity coefficient of component *i*. Substituting Eq. 2.6 into Eq. 2.5 produces:

$$\mu_i = \mu_i^* + RTlnx_i + RTln\gamma_i \tag{2.7}$$

Eq. 2.7 is equivalent to:

$$\mu_i = \mu_i^* + RT \ln(x_i \gamma_i) = \mu_i^* + RTln(a_i) \tag{2.8}$$

where a_i is the activity of component i , defined as (Thomsen 2009):

$$a_i = x_i . \gamma_i \tag{2.9}$$

If component *i* is a salt, its total activity is calculated from that of the cation and that from the anion using the following equation:

$$a_{\pm} = [(a_+)^{\nu+} . (a_-)^{\nu-}]^{1/\nu} \tag{2.10}$$

where $a_{\pm}$ is the total or mean activity of the salt; a_+ and a_- are the activities of the cation and the anion, respectively; and ν_+ and ν_- are the numbers of the moles of cations and anions in the dissociation equation, respectively. The parameter ν is the summation of the ν_+ and ν_-. Finally, for the system isopropanol(I)/water(W)/NaCl(±) at constant pressure and temperature, the equal chemical potential requirement (Eq. 2.3) can be conveniently written as:

$$a_I^O = a_I^A \tag{2.11}$$

$$a_W^O = a_W^A \tag{2.12}$$

$$a_{\pm}^O = a_{\pm}^A \tag{2.13}$$

Eq. 2.1 to 2.13 are suitable for engineering calculations as the activities of the components can be calculated using excess energy models such as the electrolyte versions of NRTL or UNIQUAC. Note, the organic and aqueous phase compositions are those that satisfy the equal activity criteria defined by Eq. 2.11 to 2.13.

2.3 Experimental Investigation of the Phase Behaviour of Alcohol/Water/Salt Mixtures

The phase behaviour of alcohol/water/salt mixtures has been extensively investigated in the last 30 years as it has potential application in the purification of alcohols produced by aqueous fermentation of biomass. The focus has been to understand the effect of variables such as the chemistry of the alcohol and the nature of ionic interactions between the salt and the other mixture components in the purity and amount of alcohol produced. The pioneering work by Frankforter and Frary (Frankforter and Frary, 1913) studied the phase behaviour of ethanol/water/salt mixtures at room conditions. Specifically, these authors investigated the effect of salts such as potassium fluoride and potassium carbonate on the liquid-liquid boundary. It was found that potassium fluoride had a very strong salting-out power compared to that of potassium carbonate. Salting-out power was defined as the capacity of a salt to separate a higher-purity alcohol from an aqueous mixture. Reber *et al.* (Reber *et al.,* 1941) studied the effect of salt content on the critical consolute temperature of butanol/water using salts such as sodium sulfate, sodium chloride, sodium bromide, sodium nitrate, sodium iodide, and sodium thiocyanate. These authors found experimentally that each one of these salts, except sodium thiocynate, increased the upper critical consolute temperature of the solution which, in terms of solubility, is equivalent to a reduction in the solubility of butanol in water. The authors pointed out that the anion plays a very important role in determining the salting-out power of the salt; however, a theoretical interpretation of this observation was not provided.

De Santis *et al.* (De Santis *et al.,* 1976) investigated the effect of the alcohol structure on the liquid-liquid equilibria of alcohol/water/NaCl mixtures. Water-soluble alcohols such as propanol, isopropanol, butanol, isobutanol, sec-butanol, and tert-butanol were investigated and the location of the liquid-liquid phase boundary and liquid-liquid phase compositions at ambient conditions were measured. Fig. 2.5 shows the mass percent of alcohol in the aqueous phase versus the mass percent of NaCl in the aqueous phase at ambient conditions (a similar figure was constructed by

the authors). The data in Fig. 2.5 shows, that, in general, the solubility of the alcohols in the aqueous phase decreases as the NaCl content in the aqueous phase increases. This result indicates that the alcohol preferentially partitions to the alcohol-rich or organic phase as the salt content increases. The lowest and highest solubilities in the aqueous phase were found for butanol and isopropanol, respectively.

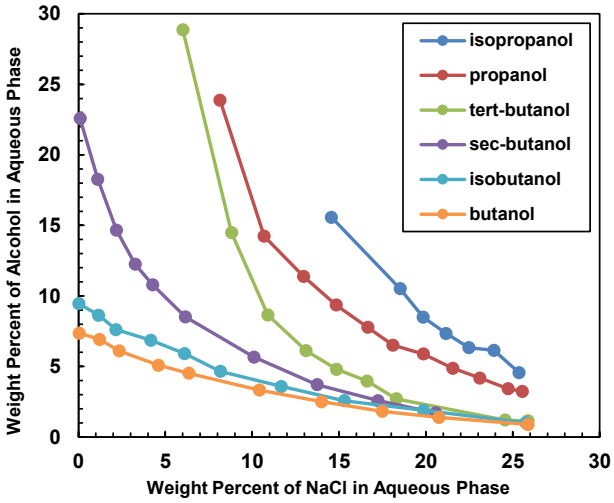

Figure 2.5. The effect of NaCl on the composition of alcohols in the aqueous phase for the liquid-liquid phase composition of alcohol/NaCl/water system at 25˚C (De Santis *et al.,* 1976).

De Santis *et al.*(De Santis *et al.,* 1976) also compared the solubility of butanol isomers in the aqueous phase. The branched isomers of butanol (tert-butanol, sec-butanol, and isobutanol) have higher solubilities in water than normal butanol (Fig. 2.5) due to differences in the effect of the hydroxyl group which tends to neutralize the hydrophobic effect of the paraffinic chain. Therefore, branched alcohols are more hydrophilic than normal alcohols of the same carbon number .(Palit, 1947; Amidonx *et al.,* 1974). These observations indicate that the liquid-liquid separation of branched alcohols from aqueous mixtures is more challenging due to the higher affinity of these components with water.

Gomis *et al.*(Gomis *et al.,* 1994(a)) studied the phase behaviour of mixtures of propanol/water/salt and isopropanol/water/salt at ambient conditions. The salts tested were NaCl and KCl and the measured triangular diagram for the mixture isopropanol/water/NaCl is presented in Fig. 2.6. The reported triangular diagrams show a single-phase liquid region at low salt content, a liquid-liquid

region, two liquid-solid regions (one liquid is rich in alcohol and the other rich in water) and one liquid-liquid-solid region. When NaCl is used, the liquid-liquid solid region is smaller for isopropanol than for propanol. Moreover, when KCl is used, the mixture of isopropanol/water/KCl does not split into two liquid phases indicating that KCL is not a suitable salt for liquid-liquid extraction of isopropanol. Comparing the results for the mixtures propanol/water/NaCl and propanol/water/KCl, the area of the liquid-liquid region is larger when NaCl is used compared to that when KCl is used. These results indicate that the Na^+ cation is capable of binding to more water molecules compared to the K^+ cation; *i.e*, the solubility of propanol in water is lower when NaCl is added to the mixture due to higher affinity between Na^+ and water molecules (Gomis *et al.,* 1994(a); Eisen and Joffe, 1966).

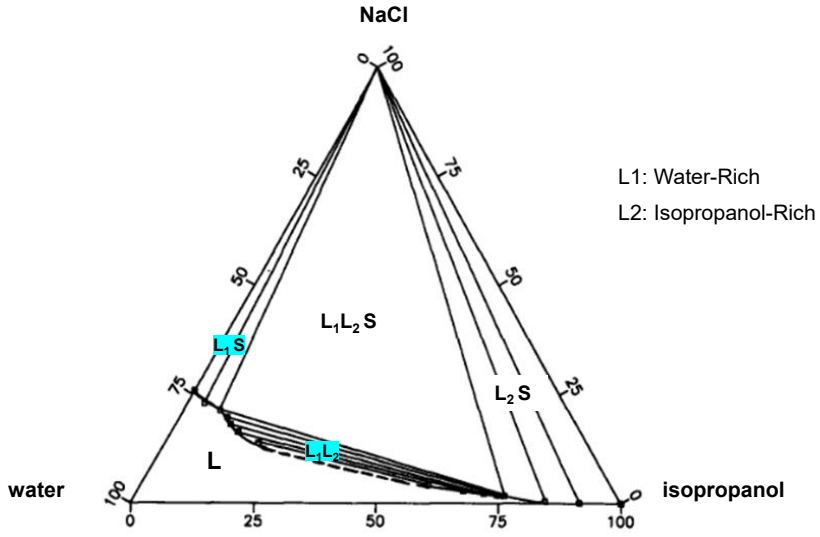

Figure 2.6. Different phase regions for the isopropanol/water/NaCl at 25 ˚C and atmospheric pressure (Gomis *et al.,* 1994(a)). L, LS and LLS stand for single liquid, liquid-solid and liquid-liquid-solid phases, respectively.

2.3.1 Liquid-Liquid Phase Boundary or Binodal Curve

Most of the studies reported in the literature on the phase behaviour of alcohol/water/salt mixtures have been focused on the experimental determination of the liquid-liquid boundary; also known as the binodal curve. At constant temperature and pressure, the binodal curve defines the composition of the mixture at which liquid-liquid phase separation is thermodynamically favorable

(Prausnitz *et al.,* 1978). Therefore, the measurement of the binodal curve is very important for the design of industrial liquid-liquid extraction operations.

The experimental method for the measurement of the binodal curve is based on turbidimetric, or cloud point titration (Merchuk *et al.,* 1998; Khayati and Gholitabar, 2016; Zafarani-Moattar *et al.,* 2019; Pimentel *et al.,* 2017). The basis of the method is the addition of water to a two-liquid phase alcohol/water/salt mixture until the turbidity, or cloudiness, due to the presence of two immiscible phases disappears. The location in the phase diagram where the solution turns transparent is the liquid-liquid boundary or binodal curve. The turbidimetric titration method has been used for detecting the binodal curve of alcohol/water/salt mixtures listed in Table 2.2. Fig. 2.7 shows the measured binodal curve for the isopropanol/water/NaCl mixture at ambient conditions (Khayati and Gholitabar, 2016). The regions below and above the binodal curve correspond to a single liquid phase (L) and two-liquid phases (LL), respectively. Liquid-liquid tie lines connect two points located on the binodal curve: one point corresponds to the alcohol-rich (organic) phase and the other to the water-rich (aqueous) phase.

Table 2.2. Summary of alcohols, salts and conditions for which the binodal curve has been measured using turbidimetric titration.

Alcohol	**Salt**	**T, ˚C**	**P, kPa**	**Ref.**
propanol, isopropanol	Choline Chloride	25, 35, 45	101	Zafarani-Moattar *et al.*
propanol, isopropanol	K_2HPO_4	25	101	Muniz *et al.*
propanol, isopropanol	KCl, NaCl, CaCl	25	101	Khayati *et al.*

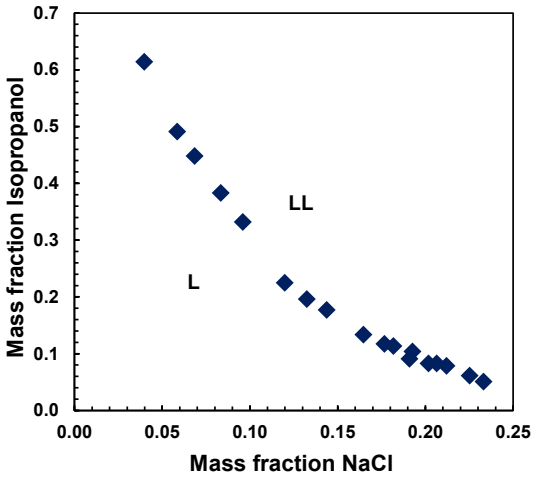

Figure 2.7. The binodal curve data for the isopropanol/water/NaCl mixture at 25˚C and atmospheric pressure measured by Khayati *et al.* (Khayati and Gholitabar, 2016). L and LL indicate the single liquid and the liquid-liquid phase regions, respectively.

The location of the binodal curve on the phase diagram of alcohol/water/salt mixtures is highly dependent on the chemistry of the alcohol, the type of salt, the temperature, and the pressure. Khayati *et al.* (Khayati and Gholitabar, 2016) measured the binodal curve at ambient conditions for ternary mixtures containing propanol or isopropanol, water, and salts such as KCl, NaCl, and $CaCl_2$. The reported data show that for the same salt, the binodal curve of the mixtures containing propanol is below that of the mixtures containing isopropanol, *i.e.*, mixtures containing propanol split into two liquid phases at lower salt content, Fig. 2.8. According to the authors, this result is consistent with the higher polarity of propanol compared to that of isopropanol which indicates that molecules of propanol tend to associate stronger with alike molecules; hence, this alcohol is separated off of the liquid mixture more easily than isopropanol that tends to interact more with the water. The authors based this interpretation on the higher dielectric constant of propanol (20.6) compared to that of isopropanol (19.4) at room temperature. Similar results were obtained by Muniz *et al.* (Muniz *et al.,* 2021). Regarding the effect of the salt, Khayati *et al.* found that, for the same alcohol, the binodal curve shifts to higher alcohol content for the salts in the following order: $CaCl_2$, NaCl, and KCl, Fig. 2.8. In addition, according to the authors, the liquid-liquid region for the mixture alcohol/water/$CaCl_2$ is bigger than those for alcohol/water/NaCl and alcohol/water/KCl, respectively. The authors found that the salting-out power (the ability of the salt to split the mixture into two liquid phases) of the salt increases with a reduction in the cation size (Khayati *et al.,* 2014). Calcium, sodium, and potassium cations have radii of 100, 102, and 138 pm, respectively (Marcus, 1991).

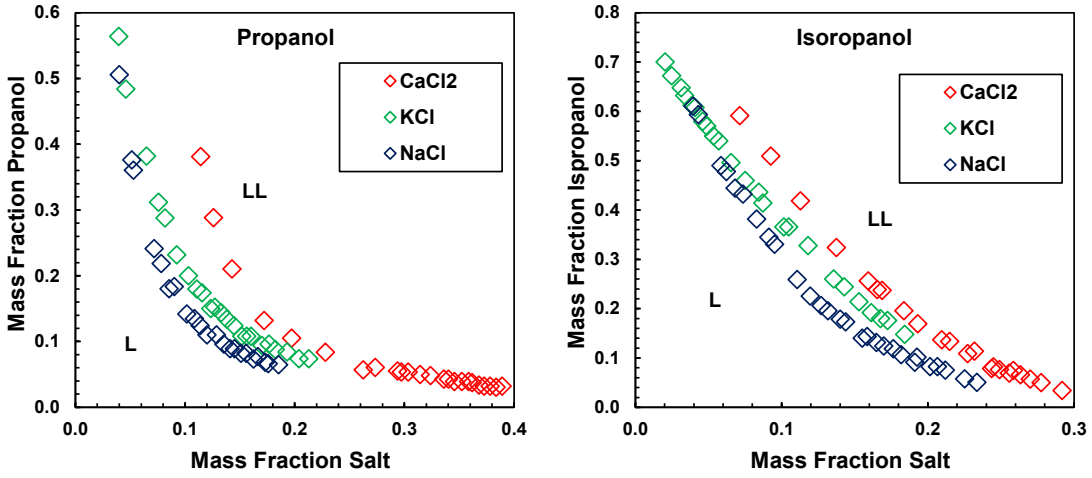

Figure 2.8. Binodal curves for (propanol/isopropanol) +(CaCl2/KCl/NaCl) +water mixture at 25˚C and atmospheric pressure. L and LL indicate the single liquid and the liquid-liquid phase regions, respectively (Khayati and Gholitabar, 2016).

The temperature also has an important effect on the location of the binodal curve in the phase diagram. Few studies have been focused on the study of the effect of the temperature on the binodal curve of mixtures of alcohol/water/salt; they are briefly discussed here. Pimentel *et al.* (Pimentel *et al.,* 2017) studied the effect of temperature on mixtures of isopropanol/water/sodium sulfate and isopropanol/water/magnesium sulfate at temperatures from 25 to 50°C at atmospheric pressure. The results show that for the mixture isopropanol/water/sodium sulfate, the liquid-liquid region widens at higher temperatures; and, for the mixture isopropanol/water/magnesium sulfate, the temperature does not have a significant effect on the liquid-liquid region. This result indicates that the phase split is driven by the change of entropy rather than by the change in the enthalpy as concluded by Nemati *et al.* (Nemati-Kande and Shekaari, 2013), Da Silva *et al.,* (Da Silva and Loh, 2000) and Martins *et al.* (Martins *et al.,* 2010). The results from other studies suggest that at temperatures from 25 to 50°C the effect of temperature on the binodal curve of alcohol/water/salt mixtures is negligible (Arzideh *et al.,* 2018; Salabat and Hashemi, 2006; Zafarani-Moattar and Jafari, 2013; Katayama and Miyahara, 2006; Hu *et al.,* 2009; Nemati-Kande *et al.,* 2012). However, changes in the temperature affect the solubility of the salt and alcohol in the water impacting the composition of the alcohol-rich and the water-rich phases without having a significant effect on the binodal curve (Katayama and Miyahara, 2006). More studies are needed to shed light on the nature of electrostatic interactions and hydrogen bonding controlling the solubility of the salt and alcohol in water, respectively.

2.3.2 Vapor-Liquid Equilibrium of Alcohol/Water/salt Mixtures

The vapor-liquid equilibrium (VLE) of alcohol/water/salt mixtures has been investigated because of its potential application in the purification of alcohol by distillation. The addition of salt to a mixture of alcohol/water increases the relative volatility of the alcohol facilitating its separation by distillation (Morrison *et al.,* 1990). The ions of the salt preferentially interact with the molecules of water creating high molecular weight structures with lower relative volatility compared to that of the alcohol (Morrison *et al.,* 1990). Moreover, for some alcohol/water mixtures, such as ethanol/water, a small addition of salt is sufficient to eliminate the azeotrope suggesting that the salt may be a useful separating agent for azeotropic distillation (Morrison *et al.,* 1990; Gomis *et al.,* 2018; Polka and Gmehling, 1994; L. Xu *et al.,* 2018). Hence mapping the vapor-liquid equilibrium of alcohol/water/salt mixtures is very important for the design, simulation, and optimization of distillation operations.

Some studies have investigated the vapor-liquid equilibrium of alcohol/water/salt mixtures, mostly at atmospheric pressure. Gomis *et al.* (Gomis *et al.,* 2018) mapped the vapor-liquid (VL), the liquid-liquid-vapor (LLV), the solid-liquid-liquid-vapor (SLLV), and the solid-liquid-vapor (SLV) regions of the phase diagram of tert-butanol/water/NaCl and tert-butanol/water/KCl at atmospheric pressure. The results show that at higher temperatures, the area of the LLV region is larger compared to that of the LL region whereas the area of the other regions is not significantly affected by the temperature. Vercher *et al.* (Vercher *et al.,* 1991) and Schmitt (Schmitt, 1979) measured the vapor-liquid equilibrium compositions of mixtures of ethanol/water/potassium acetate; and, Ohe (Ohe, 1998) and Gironi *et al.* (Gironi and Lamberti, 1995) measured the effect of adding calcium chloride, magnesium chloride, and magnesium bromide on the vapor-liquid equilibrium compositions of mixtures isopropanol/water. In general, the addition of salt to the alcohol/water mixture increases the alcohol content in the vapor phase and eliminates the azeotrope as shown in Fig. 2.9

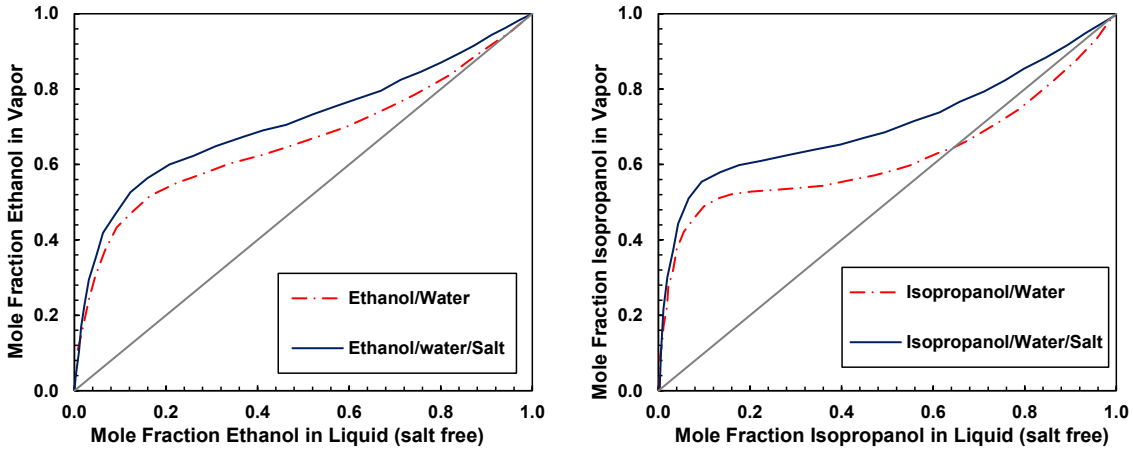

Figure 2.9. x-y diagrams for water/Ca(NO3)2/ethanol or isopropanol mixture at 50.66 kPa. The Molality of the calcium nitrate is m=1.038 mol.kg-1 for both mixtures (Polka and Gmehling, 1994).

The higher alcohol content in the vapor phase shown in Fig. 2.9. indicates that the relative volatility of the alcohol increases with the addition of salt. Xu *et al.*(L. Xu *et al.,* 2018) measured the effect of adding calcium chloride on the relative volatility of the alcohol in a mixture of allyl alcohol/water. The results shown in Fig. 2.10. indicate that adding a small amount of salt to relative volatilities significantly increases the relative volatility of the alcohol.

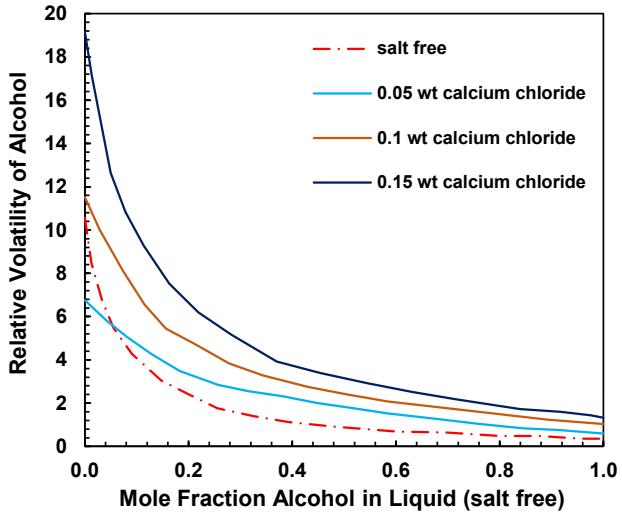

Figure 2.10. The changes in the relative volatility of allyl alcohol for three salt concentrations in water/CaCl2/allyl alcohol system at 101.3 kPa (L. Xu *et al.,* 2018).

2.4 Summary

This chapter presented a general review of the phase behaviour of alcohol/water/salt systems. The addition of salt to a binary mixture of alcohol/water triggers a liquid-liquid phase separation with one of the phases being rich in alcohol and the other in the water. Additionally, depending on the amount of salt added, the system could exhibit liquid-solid or liquid-liquid-solid regions. The liquid-liquid region of the phase diagram has been widely studied; however, very few studies have focused on investigating the effect of temperature on this region. The addition of salt to a binary alcohol/water has also an effect on the vapor-liquid equilibrium of the system. The presence of salt increases the relative volatility of the alcohol and consequently the alcohol content in the vapor phase increases. Another important effect of the salt is the elimination of the azeotrope in the case of azeotropic alcohol/water mixtures.

Despite the data reported in the literature on the phase behaviour of alcohol/water/salt systems, there are no comprehensive studies on the different regions of the phase diagram. The liquid-liquid and vapor-liquid regions have been considered separately and regions such as the vapor-liquid-liquid, vapor-liquid-liquid-solid, and vapor-liquid-solid have not been systematically studied. Moreover, the effect of important process variables such as temperature and pressure on the phase behaviour of these mixtures has not been studied. Therefore, as a preliminary study, this research is focusing on studying the effect of the temperature on the liquid-solid, liquid-liquid and liquid-liquid-solid regions of the phase diagram of the isopropanol/water/NaCl mixture. Also, the effect of the addition of salt on the normal boiling point of the mixture and vapor-liquid phase compositions was studied. The outcome is a comprehensive and thermodynamic consistent dataset that helps in the understanding of the phase behaviour of isopropanol/water/NaCl mixtures.

Chapter 3: Experimental Method

This chapter presents all the experimental methods used in this study to map the phase behaviour of isopropanol/water/NaCl mixtures at atmospheric pressure. First, it presents general information about the chemicals used and about the preparation of the samples for the experiments. Second, a description of the experimental procedures to measure liquid-liquid-solid and liquid-liquid boundaries is presented as well as a description of the experimental devices used. Third, a description of the experimental procedure to measure liquid-liquid phase compositions is presented; and, finally, the procedure and apparatus to measure boiling points are described. In addition, an analysis of the errors of the different procedures is presented as well as the validation of the experimental procedures.

3.1 Materials

The chemicals used for the preparation of the mixtures were deionized water, isopropanol (purity 99.5%), and sodium chloride (purity 99%). Isopropanol and sodium chloride were purchased from Fisher Scientific.

3.2 Sample Preparation

Mixtures of isopropanol, water, and sodium chloride were prepared at ambient temperature and atmospheric pressure. Prior to the preparation of the mixtures, and to eliminate any moisture, the sodium chloride was dried in an oven at a temperature of 82°C for at least two hours and then placed inside a desiccator (containing silica gel) until it reached ambient temperature. Then, known masses of isopropanol, water, and salt were placed in a flask equipped with a total reflux condenser and magnetic stir bar and agitated at ambient temperature. The total reflux condenser was needed to avoid the evaporation of isopropanol. Cold water was used as a coolant. The masses of the chemicals were determined using a Mettler Toledo analytical balance with a readability of 0.0001g.

3.3 Liquid-Liquid-Solid and Liquid-Liquid Phase Boundary Measurements

The liquid-liquid-solid (LLS) and the liquid-liquid (LL) phase boundaries were measured using the setup shown in Fig. 3.1 This setup consists of a 250 mL 3-neck flask equipped with a thermocouple, a condenser, and a separatory funnel. The flask was enclosed in a temperature-controlled air bath used to control the temperature of the sample in the flask within ±0.1 °C of the intended measurement temperature. The temperature of the sample was measured with a K-type thermocouple calibrated against a platinum resistance thermometer (PRT). This thermocouple was in direct contact with the sample as shown in Fig. 3.1. To avoid the evaporation of volatile components, the condenser was connected to a temperature-controlled circulating bath that used ethylene glycol at 0°C as the coolant. The separatory funnel was charged with deionized water and was used during the measurement to add water to the sample. The setup was open to the atmosphere; therefore, only measurements at atmospheric pressure were collected.

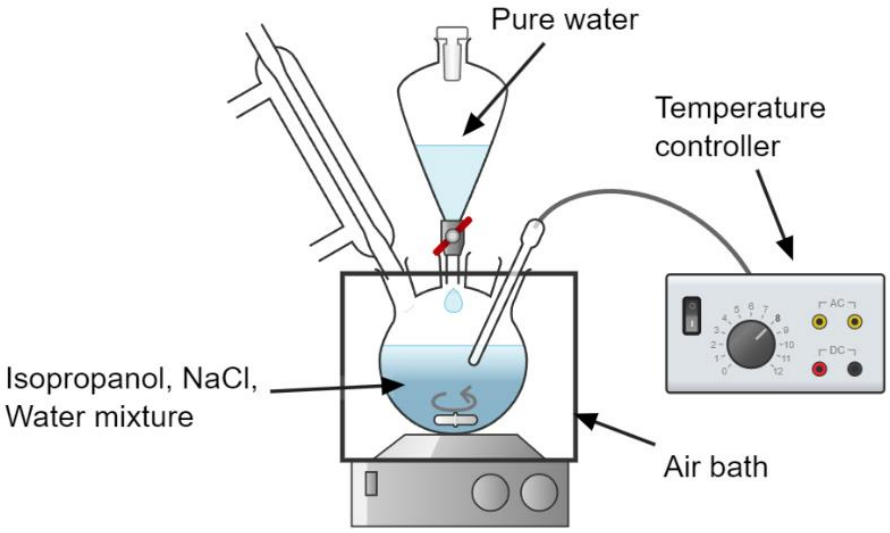

Figure 3.1. Experimental setup for the titration experiment to determine the phase boundaries of isopropanol/water/NaCl mixture at atmospheric pressure.

To begin an experiment, the setup was placed on top of a magnetic stirrer plate, and a magnetic stir bar was placed inside the flask to ensure agitation during the experiment. Then, approximately 100 mL of a tree-phase (solid-liquid-liquid) sample containing isopropanol, water, and sodium chloride was charged into the flask at ambient temperature and agitated during the entire length of the measurement. Once the temperature of the sample was at the intended measurement value, the deionized water contained in the separatory funnel was added dropwise to the three-phase sample

until the disappearance of the solid phase. The disappearance of the solid phase was visually detected. The deionized water was added slowly enough to avoid any changes in the temperature. In cases when the temperature of the sample changed, the separatory funnel valve was closed, and the system was allowed to go back to the measurement temperature before resuming the measurement. The mass of deionized water added to the disappearance of the solid phase was measured and the composition of the sample was calculated from a mass balance using the initial masses of isopropanol, sodium chloride, and deionized water; and the mass of deionized water added. The calculated value is the composition of the sample at the LLS boundary. At the LLS boundary only the two liquid phases were left, and, due to the agitation, one phase was dispersed into the other and the system was visibly turbid. More deionized water was slowly added to the sample until the solution was translucid which indicated only one single liquid phase was left in the system. At this moment, the mass of deionized water was measured and the composition at the LL boundary was calculated as described for the LLS boundary. The procedure described here for detecting the LL boundary as the transition between a turbid and translucid solution was adapted from that proposed elsewhere (Gomis *et al.,* 1994(a); Pirdashti *et al.,* 2015; Khayati and Gholitabar, 2016; Pimentel *et al.,* 2017; Muniz *et al.,* 2021; Merchuk *et al.,* 1998).

3.3.1 Validation of the Procedure

The experimental procedure described in Section 3.3 for the measurement of the LL phase boundary was validated using data from the literature reported at room temperature and atmospheric pressure. A similar validation for the procedure to measure the LLS boundary was not possible as data have not been reported. Fig. 3.2 shows the experimentally measured LL phase boundary for the isopropanol/water/NaCl mixture at room temperature and the data reported by Khayati *et. al* (Khayati and Gholitabar, 2016), for the same mixture at room temperature. Because the data collected in this study and that from the literature were measured at different sodium chloride contents, as shown in Fig. 3.2, an empirical correlation was fitted to the data collected in this study. The purpose of fitting this correlation to the collected data was to make the comparison easier and to allow the calculation of the deviations required to validate the experimental methodology proposed in this study. The empirical correlation used to fit the collected data at room temperature is given by:

$$wt_{isopropanol} = exp(-18.472wt_{NaCl}^2 - 7.761wt_{NaCl} - 0.170) \quad (3.1)$$

where $wt_{isopropanol}$ and wt_{NaCl} are the experimental mass fractions of isopropanol and sodium chloride, respectively. The calculated mass fractions of isopropanol from Eq. 3.1 were within 0.6% of the experimentally measured data and 2% of reported values. The repeatability of the measurements was ±3%.

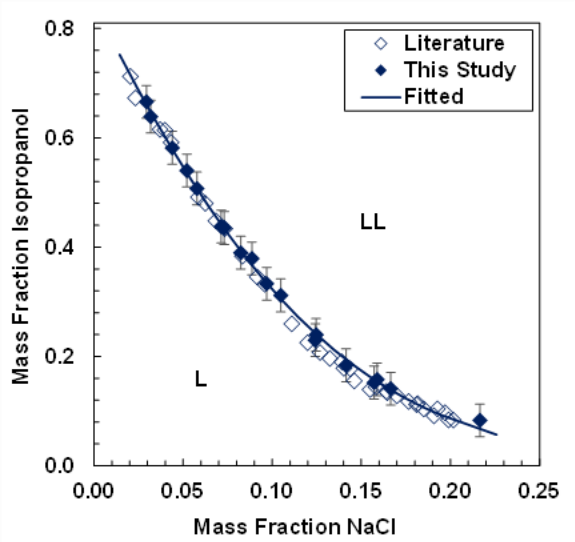

Figure 3.2. Binodal curve for the mixture of isopropanol/water/NaCl at ambient temperature and atmospheric pressure. L and LL indicate the single liquid and the liquid-liquid phase regions, respectively. The data from the literature was collected from Khayati *et al.* (Khayati and Gholitabar, 2016).

3.4 Measurement of Liquid-Liquid Phase Compositions

The setup used for collecting samples from the two liquid phases at thermodynamic equilibrium was the same one described in Section 3.3 but without the separatory funnel. Instead, the mouth to which the separatory funnel was attached, was plugged using a glass stopper to avoid the evaporation of either isopropanol or water during the experiment. The sample was not agitated during this experiment. To begin the experiment, approximately 100 mL of a two-liquid phase mixture containing isopropanol, water, and sodium chloride was charged into the flask and let to reach equilibrium at the intended measurement temperature, typically for three days. During this period, the temperature of the solution fluctuated within ±0.1°C. Then, approximately 5 mL aliquots from the two liquid phases at equilibrium were extracted from the flask using syringes. Then, the samples collected from the organic (alcohol-rich) and the aqueous (water-rich) phases

were transferred to airproof glass vials. Liquid-liquid phase compositions were measured at 0, 21, 50, and 70°C at atmospheric pressure using this procedure.

The NaCl, isopropanol, and water mass content in both phases were determined according to the following procedure. An aliquot of approximately 10 g of the liquid phase was weighed in the analytical balance described in Section 3.2. The volatile components in this aliquot, isopropanol and water, were evaporated from the aliquote and then condensed using the setup shown in Fig. 3.3. The temperature in the condenser was kept around 0°C to ensure the total condensation of the volatile components. The condenser was connected to a temperature-controlled circulating bath that used ethylene glycol as the coolant. The residue, assumed to be pure NaCl, was then dried in an oven at 82°C for 2 hours and let cool inside a moisture-free desiccator before weighing. The mass fraction of NaCl in the phase was calculated as the mass of the residue divided by the mass of the aliquot.

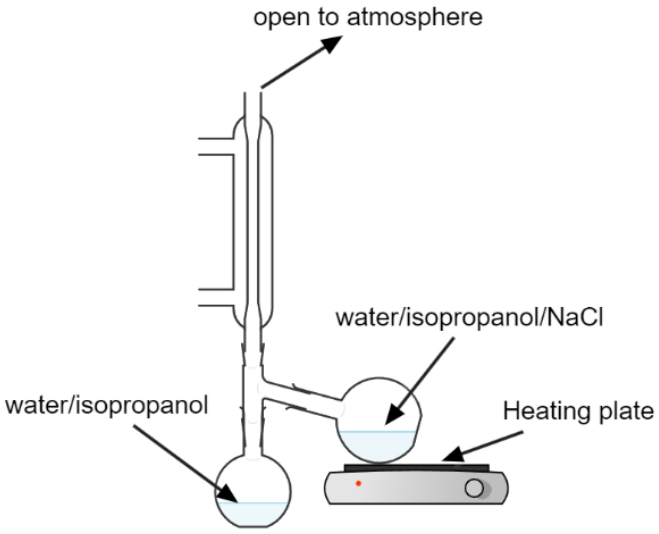

Figure 3.3. Experimental setup used in the determination of the NaCl content in the aliquots.

The collected condensate, assumed to contain only isopropanol and water, was weighed and its composition was determined from its refractive index at 25°C. For this purpose, a calibration curve was constructed by measuring the refractive indexes of several samples prepared by mixing known masses of isopropanol and water. The refractive indexes were measured in a Reichert Abbe Mark III refractometer with accuracy of ± 0.01%. The calibration curve used in this study is shown in

Fig. 3.4 and the data were fitted using the correlation proposed by Yarranton *et al.* (Yarranton *et al.,* 2015) for binary mixtures:

$$\frac{1}{RI_{mix}} = \frac{w_1}{RI_1} + \frac{w_2}{RI_2} - w_1 w_2 \left(\frac{1}{RI_1} + \frac{1}{RI_2}\right) \beta_{12}^* \qquad (3.2)$$

where *RI* is the refractive index; *w* is the mass fraction ($w_1 + w_2 = 1$); and subscripts *mix*, *1* and *2* refer to the binary mixture, isopropanol, and water, respectively. β_{12}^* is a binary interaction parameter calculated by fitting Eq. 3.2 to data. In this study, $\beta_{12}^* = 0.0199$. The measured refractive indexes used for the construction of the calibration curve were within 0.05% of the reported values from the NIST Database (National Institute of Standard and Technology (NIST), 2008). All the refractive indexes collected in this study were measured at 25°C and atmospheric pressure.

The isopropanol mass fraction in the condensate was calculated from Eq. 3.2 using the measured refractive index of the condensate and the refractive indexes of pure isopropanol and water as inputs. Finally, the mass fraction of isopropanol in the phase was calculated by multiplying the calculated mass fraction of isopropanol in the condensate by the measured mass of the condensate and dividing the result by the mass of the aliquot. The mass fraction of water in the phase was calculated from the mass balance using the calculated mass fractions of NaCl and isopropanol as inputs.

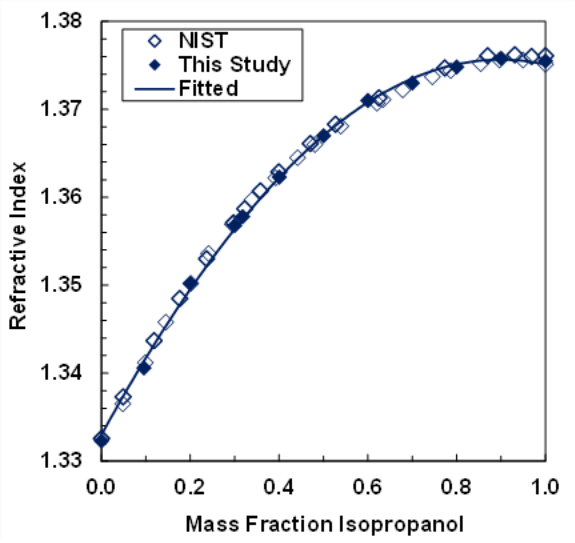

Figure 3.4. The calibration curve plotted by Eq. 3.2 by fitting the reported data from NIST (National Institute of Standard and Technology (NIST), 2008)and the experimental data for the refractive index of water/isopropanol mixture at 25 ˚C.

3.4.1 Validation of the Procedure to Measure Liquid Phase Compositions

The procedure used in this study to measure the composition of the liquid phases was validated as follows. Four standard solutions of known composition were prepared by mixing known masses of isopropanol, water, and NaCl at room temperature and atmospheric pressure. The compositions of these four standard solutions were chosen to cover the entire range of composition along the LL boundary shown in Fig. 3.2, but slightly below this boundary to ensure a single liquid phase. The mass composition of each one of the standard solutions was measured as described in Section 3.4. Fig. 3.5 shows a scatter plot comparing the mass fraction composition of the standard solutions with those measured according to the procedure described in Section 3.4. The calculated average relative deviations for the measured mass fractions of isopropanol, NaCl, and water were 5, 2, and 1%, respectively.

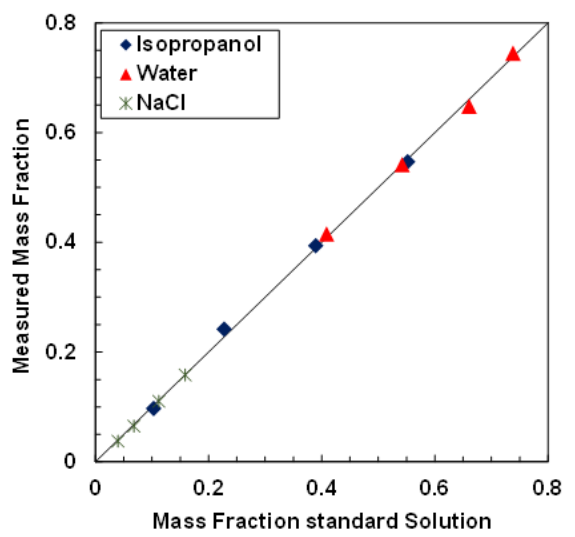

Figure 3.5. The dispersion plot compares the mass fraction of the mixture by the evaporation procedure with the mass fraction of the standard solution.

3.4.2 Thermodynamic Consistency Check for Measured Liquid Phase Compositions

To ensure the measured LL phase compositions are thermodynamically consistent with the definition of thermodynamic equilibrium, these data must obey the Gibbs-Duhem equation (Prausnitz *et al.,* 1978). At constant temperature and pressure, the Gibbs-Duhem equation is given by:

$$\sum_i x_i d\ln\gamma_i = 0 \tag{3.3}$$

where x and γ are the mole fraction and activity coefficient of component i, respectively. However, in the case of liquid-liquid equilibrium, the activity coefficients of the components cannot be calculated from the experimental data; rather, a ratio of activity coefficients:

$$\frac{(\gamma_i)^O}{(\gamma_i)^A} = \frac{x_i^A}{x_i^O} \tag{3.4}$$

where superscripts O and A refer to the organic and the aqueous phase, respectively. Eq. 3.4 is the equal fugacity criteria for liquid-liquid equilibrium written in terms of activity coefficients. Therefore, it is not possible to apply the Gibbs-Duhem equation to assess the thermodynamic consistency of liquid-liquid equilibrium data. Different semi-empirical approaches have been proposed to check the consistency of liquid-liquid data. The graphical approaches proposed by Hand (Hand, 1929), Bachman (Bachman, 1940), and Othmer-Tobias (Othmer and Tobias, 1942) have been widely used to test the consistency of liquid-liquid data (Pimentel *et al.,* 2017; Zafarani-Moattar *et al.,* 2019; Khayati and Gholitabar, 2016) and were used in this study. The idea behind these three approaches is simple: when the variables X and Y are plotted using consistent liquid-liquid equilibrium data, the resulting trend is linear. This linear trend is totally empirical and has been verified by a large number of mixtures; although, there is not rigorous thermodynamic proof. The variables X and Y for each approach are listed in Table 3.1. In this study, the consistency approaches proposed by Hand, Bachman, and Othmer-Tobias were used to assess the consistency of the measured liquid-liquid phase compositions.

Table 3.1. The equation to calculate X and Y parameters for Bachman, Hand, and Othmer-Tobias methods to check the thermodynamic consistency of phase composition data for the ternary mixtures at liquid-liquid equilibrium.

Method	***X***	***Y***
Bachman	$wt_{water}^{Aqueous}$	$\frac{wt_{water}^{Aqueous}}{wt_{isopropanol}^{Organic}}$
Hand	$log\left(\frac{wt_{NaCl}^{Organic}}{wt_{isopropanol}^{Organic}}\right)$	$log\left(\frac{wt_{NaCl}^{Aqueous}}{wt_{water}^{Aqueous}}\right)$
Othmer-Tobias	$log\left(\frac{wt_{isopropanol} + wt_{NaCl}}{wt_{water}}\right)_{Aqueous}$	$log\left(\frac{wt_{water} + wt_{NaCl}}{wt_{isopropanol}}\right)_{Organic}$

Fig 3.6 shows the Hand, Bachman, and Other-Tobias plots with X and Y calculated using measured and reported in literature phase compositions at room temperature and atmospheric pressure. The phase compositions measured in this study follow a linear trend with correlation coefficients, R^2, higher than 0.99; however, the data reported in the literature are scattered and only a few data points follow a straight line. These results indicate that the phase compositions measured in this study according to the procedure described in Section 3.4 satisfy the consistency check required by the approaches by Hand, Bachman, and Other-Tobias.

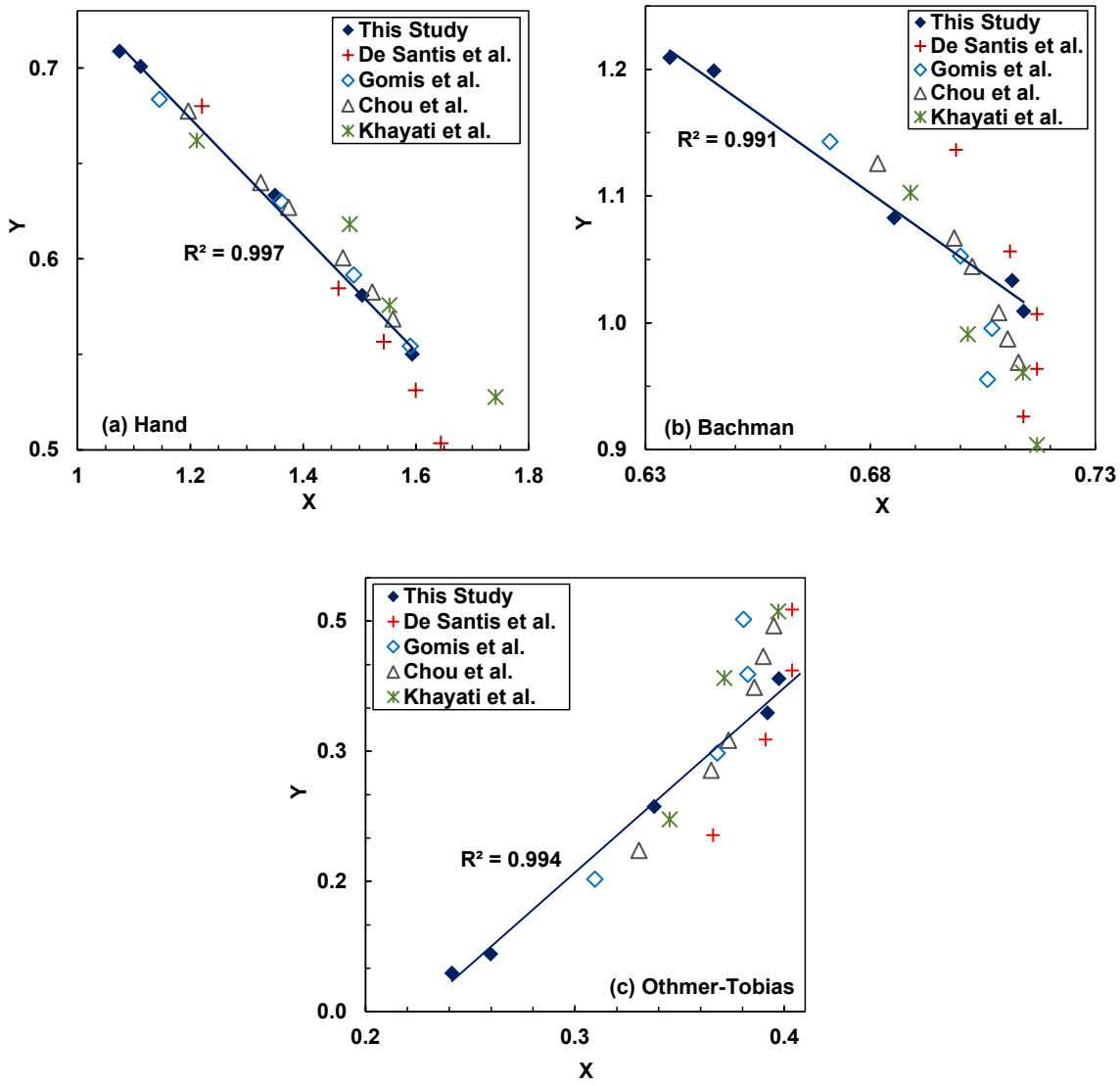

Figure 3.6. The consistency check for the experimental LL phase composition data and the reported composition data from Khayati *et al.* (Khayati and Gholitabar, 2016), Gomis *et al.* (Gomis *et al.,* 1994(a)), Chou *et al.* (Chou *et al.,* 1998), and De Santis *et al.* (De Santis *et al.,* 1976).

The measured phase compositions in this study were subjected to an additional consistency check. At thermodynamic equilibrium at constant temperature and pressure, the mass compositions of the organic and aqueous phases must fall on the LL phase boundary; and, the tie-lines, connecting the compositions of the organic and aqueous phases, must not intersect. Fig. 3.7 shows the binodal curve for the mixture of isopropanol/water/NaCl at room temperature and atmospheric pressure. The solid line corresponds to Eq. 3.1, fitted to the measured LL boundary as described in Section 3.3.1; the solid symbols correspond to the measured phase compositions, and the dotted lines are tie-lines. In general, measured phase compositions fall on the LL boundary within the error of the measurement and tie-lines do not intersect. This additional check corroborates the results obtained from the Hand, Bachman, and Other-Tobias tests and confirms the measured data at room temperature and atmospheric pressure is thermodynamically consistent. All the measured phase compositions in this study were subjected to the Hand, Bachman, and Other-Tobias tests and compared to measured LL boundaries as described here.

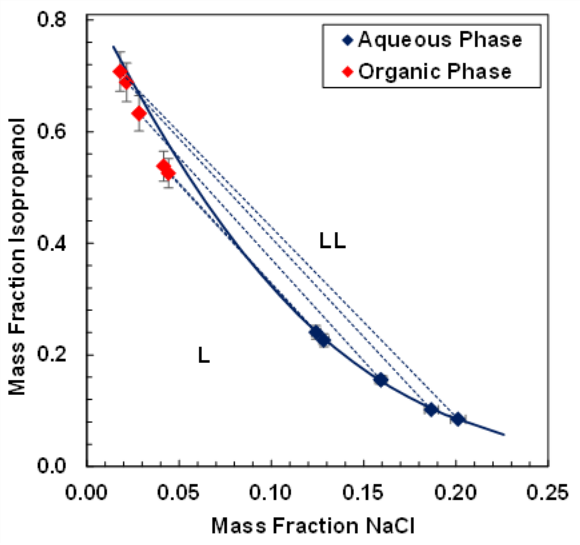

Figure 3.7. Binodal curve for isopropanol/water/NaCl mixture. (♦) shows organic phase composition, (♦) represents aqueous phase composition, and (---) are the tie-lines. All data were collected at room temperature and atmospheric pressure. L and LL indicate the single liquid and the liquid-liquid phase regions, respectively.

3.5 Measurement of Vapor-Liquid Phase Compositions

Saturation (or boiling point) temperatures and samples of the vapor and liquid phases at equilibrium were collected at atmospheric pressure using the apparatus shown in Fig. 3.8. Details of this apparatus are given elsewhere (Rogers *et al.,* 1947). Briefly, the apparatus is an ebulliometer

equipped with a Cottrell pump, a platinum resistance thermometer (precision ±0.1°C), a condenser, and a 3-way stopcock for sample collection. To begin an experiment, approximately 180 mL of a mixture of known composition are charged into the apparatus at room temperature. The apparatus is placed on a heating plate and the temperature is increased until the Cottrell pump ejects a vigorous stream of liquid over the thermometer and the condensed vapor returns from the condenser at a steady rate. During this stage, the condenser is kept at a temperature of around 0°C, and the 3-way stopcock is set to ensure total reflux of the condensed vapor. Then, the system is allowed to reach equilibrium. The system is at equilibrium when the temperature read by the platinum resistance thermometer is constant for at least 2 hours. Finally, samples of the liquid and vapor are withdrawn by manipulating the 3-way stopcock. The composition of the two phases was determined using the procedure described in Section 3.4.

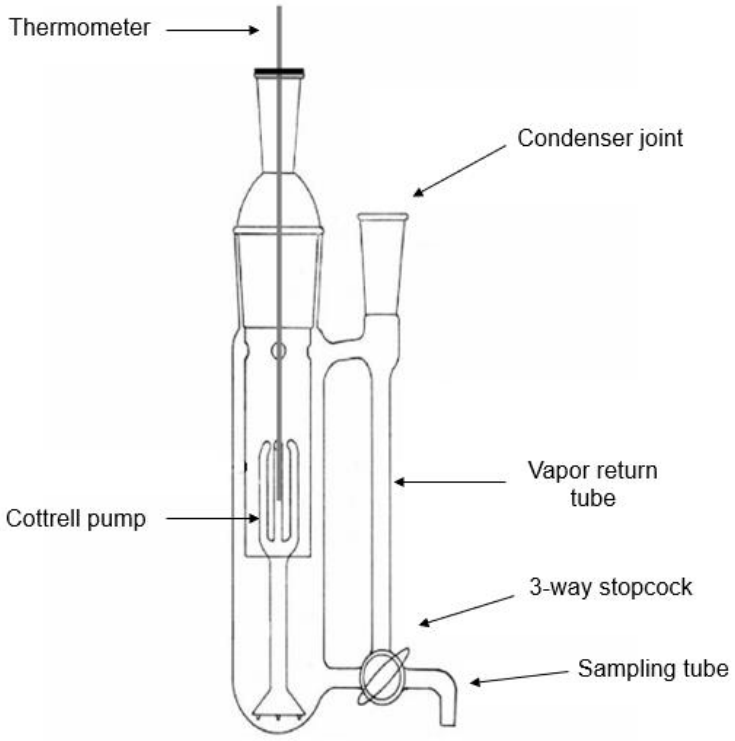

Figure 3.8. Ebulliometer used to measure the phase composition of VLE of isopropanol/water/NaCl mixture at atmospheric pressure.

3.5.1 Validation of the Procedure to Measure Vapor-Liquid Phase Compositions

The procedure for measuring saturation temperatures and vapor-liquid phase compositions was validated by measuring: 1) the boiling point and vapor-liquid phase compositions for isopropanol/water mixtures; and 2) the boiling point of NaCl/ water mixtures at atmospheric pressure. The results for isopropanol/water are presented first and then those for NaCl-water.

Isopropanol/Water Mixtures: saturation temperatures and vapor and liquid phase compositions were measured at atmospheric pressure using the apparatus and procedure described in Section 3.5. Fig. 3.9 shows the measured *Txy* (Panel A) and *xy* (Panel B) diagrams for the isopropanol/water mixture at atmospheric pressure. For comparison, the vapor-liquid equilibrium of the mixture was modeled using a γ-ϕ approach with activity coefficients (γ) calculated from the UNIQUAC model and fugacity coefficients (ϕ) calculated from the Virial equation of state truncated after the second term as described elsewhere (Ramos-Pallares, 2023). Fig. 3.9 shows that there is a good agreement between measured and calculated liquid phase compositions with an overall average absolute relative deviation of 0.1 %. However, there is some scatter in the measured vapor phase compositions possibly because of either contamination due to mixing with the liquid phase or losses of volatile components through the condenser. The calculated uncertainties for the measured vapor mol fraction phase compositions and temperatures were ± 0.018 and ± 0.5°C, respectively, with a confidence interval of 95%.

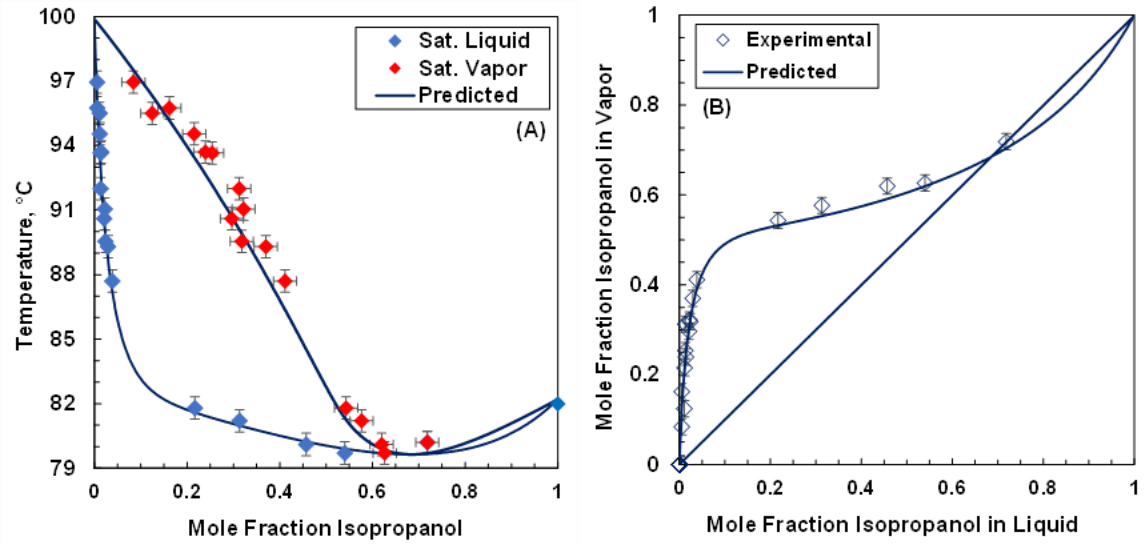

Figure 3.9. (A): Liquid phase composition (♦) and vapor phase composition (♦) for VLE of isopropanol/water mixture at atmospheric pressure. The solid line (–) was predicted by UNIQUAC model using the reported data from NIST (National Institute of Standard and Technology (NIST), 2008). (B):

Comparison of the mole fraction of isopropanol in vapor and liquid phase for isopropanol/water mixture at atmospheric pressure. The solid line (–) was predicted by UNIQUAC model using the reported data from NIST.

NaCl/Water Mixture: The boiling point of NaCl/Water mixtures was measured using the apparatus described in Section 3.5. Fig 3.10 shows reported, measured, and predicted normal boiling point temperatures of NaCl/Water mixtures. The solid line corresponds to the normal boiling points predicted from the electrolyte version of the UNIQUAC model at 97 kPa (in situ average atmospheric pressure) with the parameters reported by Thomsen (Thomsen 1997(a)). The overall absolute relative deviation between measured and predicted boiling point temperatures was 2%. The measured boiling point temperatures collected in this study according to the described procedure are slightly below predicted and reported values probably because the local atmospheric pressure fluctuates between 93 and 101 kPa.

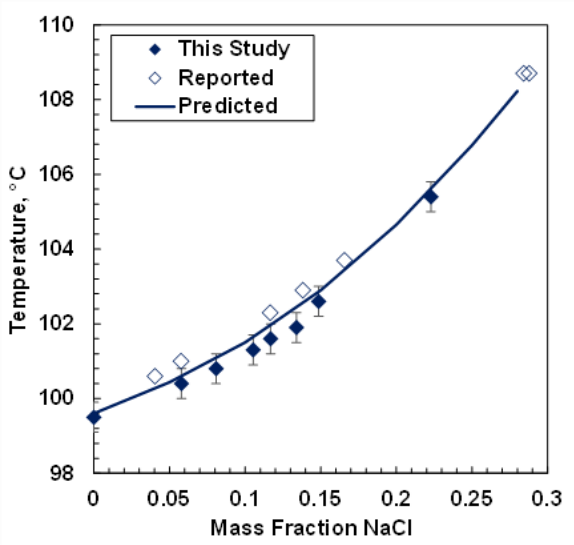

Figure 3.10. Boiling points of NaCl/water mixture at atmospheric pressure. The solid line corresponds to calculated boiling points from the electrolyte version of the UNIQUAC model as presented by Thomsen (Thomsen 1997(a)).

Chapter 4: Results and Discussion

This chapter presents a detailed analysis of the experimental phase behaviour data collected in this study for isopropanol/water/NaCl mixtures at atmospheric pressure. The data presented and analyzed here includes liquid-liquid, liquid-solid, liquid-liquid-solid, and liquid-vapor phase boundaries as well as liquid-liquid and liquid-vapor phase compositions.

4.1 Triangular Representation of the Phase Behaviour of the Mixture Isopropanol/Water/NaCl

Fig. 4.1 shows the triangular representation of the phase behaviour of the mixture isopropanol/water/NaCl at 21, 50, and 70°C at atmospheric pressure. The collected experimental data are not shown in the diagram to avoid clutter. Instead, the data corresponding to phase boundaries were fit to empirical correlations shown as solid lines. The dashed lines in Fig. 4.1 were not fitted to data, as no data along these boundaries were collected, but rather estimated by drawing a line from the point where all solid lines intersect to the vertex corresponding to pure NaCl (assuming the solid phase is pure salt). The region labelled as L in the triangular diagram corresponds to a single liquid phase. The regions labelled L_1S and L_2S correspond to a water-rich liquid (L_1) phase at equilibrium with a solid phase and to an isopropanol-rich liquid (L_2) phase at equilibrium with a solid phase (assumed to be pure solid NaCl). In the region labelled as L_1L_2S there are two liquid phases and one solid phase at equilibrium; and, finally, the region labelled as L_1L_2 corresponds to the liquid-liquid envelope. Details about the L_1S, L_2S, and L_1L_2 regions and the effect of temperature on these phase boundaries are provided in the following sections.

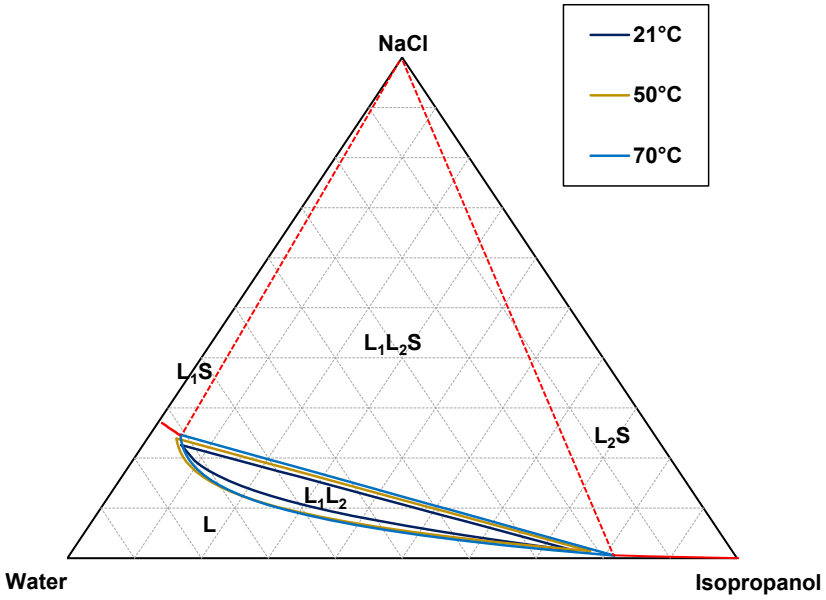

Figure 4.1. Triangular diagram for isopropanol/water/NaCl mixture at 21, 50, and 70˚C and atmospheric pressure. L_1 and L_2 are the representations for water-rich and isopropanol-rich phases respectively. L is the region with a single liquid phase and S is the solid phase.

4.2 Liquid-Solid Regions

The effect of the temperature on the boundaries between the L_1S (L_1: water-rich liquid) and L regions; and, between the L_2S (L_2: isopropanol-rich liquid) and L regions at atmospheric pressure is shown in Fig. 4.2 in panels a and b, respectively, using triangular coordinates. As the temperature increases from 21 to 50°C, the L_1S/L boundary (Fig. 4.2a) shifts toward higher NaCl mass content indicating the solubility of NaCl in the system increases with the temperature. However, the L_1S/L boundary is not affected significantly as the temperature increases from 50 to 70°C indicating the system has reached its maximum NaCl saturation. The effect of temperature on the L_2S/L boundary (Fig. 4.2b) cannot be assessed as not enough data along this boundary was collected due to experimental limitations.

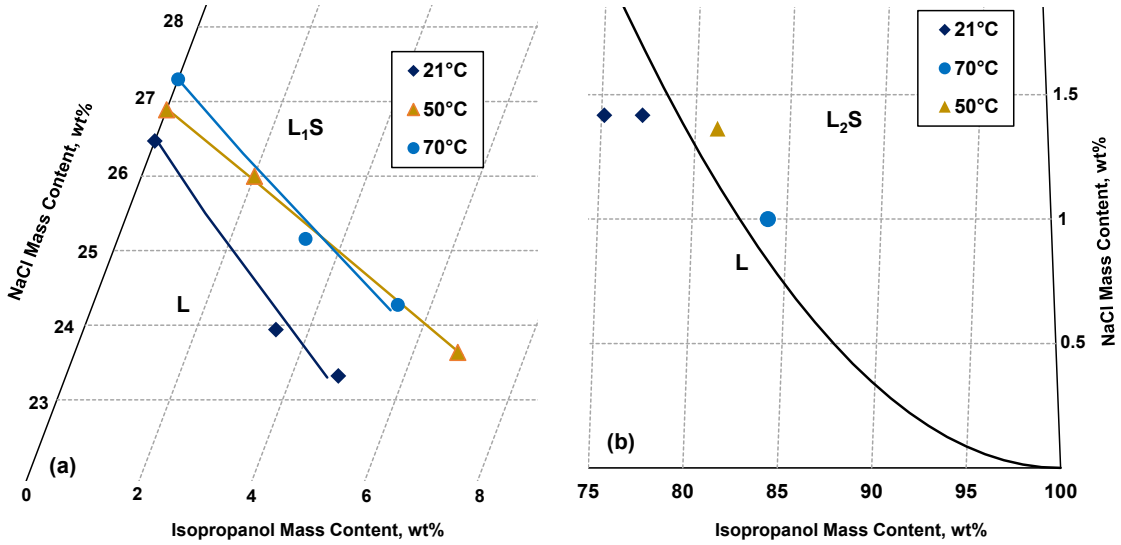

Figure 4.2. (a) The isopropanol and NaCl compositions for isopropanol/water/NaCl mixture along the L_1S and L phase boundary. (b) The isopropanol and water compositions for isopropanol/water/NaCl mixture along the L_2S and L phase boundary. All data points are collected at 21, 50, and 70˚C and atmospheric pressure. The solid lines were fit to the data and were included as visual aids. The constant water content lines were not included to avoid confusion.

4.3 Liquid-Liquid and Liquid-Liquid-Solid Regions

The boundaries of the liquid-liquid (L_1L_2) and the liquid-liquid-solid (L_1L_2S) regions for the mixture of isopropanol/water/NaCl were measured at 21, 50, and 70°C at atmospheric pressure, according to the experimental procedure described in Section 3.3. Fig. 4.3 shows the measured L_1L_2 and L_1L_2S boundaries. The collected data is presented in the Appendix A. To help in the analysis of the results, the solid lines in Fig. 4.3 correspond to Eq. 4.1 and 4.2 fitted to the measured L_1L_2 and L_1L_2S phase boundaries, respectively. Eq. 4.1 and 4.2 are empirical and were chosen because they were suitable to fit the data. These equations are given by:

$$wt_{isopropanol} = \exp\left(A * wt_{NaCl}^2 + B * wt_{NaCl} + C\right) \quad (4.1)$$

$$wt_{isopropanol} = D * wt_{NaCl} + E \quad (4.2)$$

where $wt_{isopropanol}$ and wt_{NaCl} are the isopropanol and NaCl mass fractions at the phase boundary; and A, B, C, D, and E are temperature-dependent parameters calculated by fitting the equations to data. Eq. 4.1 fitted the L_1L_2 boundary data with an overall average absolute relative deviation (AARD) of 3%. Eq. 4.2 fitted the L_1L_2S boundary data with an overall AARD of 2.7 %. The fitted temperature-dependent parameters A, B, C, D, and E are presented in Table 4.1.

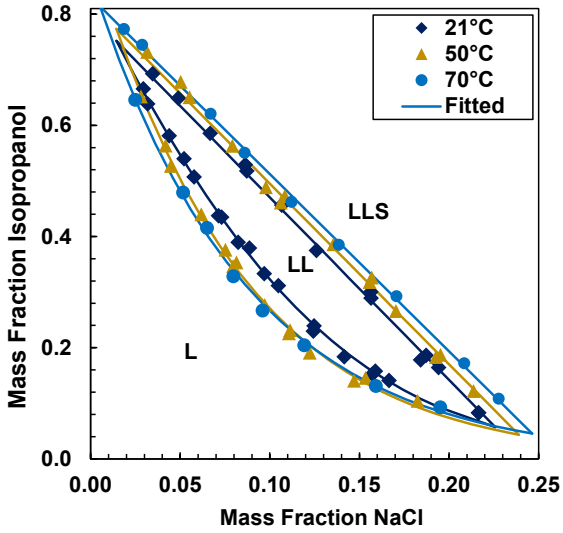

Figure 4.3. L_1L_2 and L_1L_2S phase boundaries at 21, 49.7, and 70˚C and atmospheric pressure. L, LL, and LLS respectively represent the single liquid region, liquid-liquid region, and liquid-liquid-solid region at equilibrium. Solid lines are plotted by fitting the experimental data with Eq. 4.1 and 4.2.

Table 4.1. The values of the fitting parameters for the L_1L_2 and L_1L_2S phase boundaries at 21, 49.7, and 70˚C and atmospheric pressure.

T, °C	A	B	C	D	E
21	-18.472	-7.761	-0.170	-3.285	0.799
49.7	-3.917	-11.828	-0.086	-3.250	0.820
70.0	-1.118	-11.676	-0.145	-3.187	0.831

The results presented in Fig. 4.3 show that the area of the L_1L_2 envelope slightly widens as the temperature increases from 21 to 50°C. However, the area of the L_1L_2 envelope does not widen significantly when the temperature is increased from 50 to 70°C. Considering that the solubility of NaCl in isopropanol is negligible (De Santis *et al.,* 1976), then, the area of the L_1L_2 envelope is controlled by the solubility of NaCl in water. The solubility of NaCl in water changes very little with temperature because of the formation of highly stable hydrated sodium cations (Na^+) and chlorine anions (Cl^-). The presence of these hydrated, or solvated, ions disturb the hydrogen bonding configuration of the water molecules not associated with the ions reducing the ability of this "free-water" to dissolve more NaCl at higher temperatures (Bharmoria *et al.,* 2012; Marcus, 1991). Moreover, the distortion in the hydrogen bonding configuration among these "free-water" molecules may substantially affect the solubility of isopropanol in the system. Considering that the number of "free-water" molecules does not change with temperature (because the solubility of

NaCl in water is almost temperature-independent), then, the solubility of isopropanol may be proportional to the number of "free-water" molecules which changes little with temperature; consequently, the solubility of isopropanol in the system changes slightly with the temperature. This interpretation suggests that the area of the liquid-liquid envelope for isopropanol/water/NaCl mixtures may be controlled by the radius of the solvation shell around the ions.

4.3.1 Liquid-Liquid Tie Lines

The mass compositions of the water-rich, or aqueous (L_1), and the isopropanol-rich, or organic (L_2), liquid phases were measured at 0, 21, 50, and 70°C at atmospheric pressure following the procedure described in Section 3.4. Fig. 4.4 shows the measured phase compositions and tie-lines as well as the L_1L_2 envelope calculated from Eq. 4.1 and 4.2 with the parameters summarized in Table 4.1. The L_1L_2 envelope at 0°C is not shown as no phase boundaries were measured at this temperature. The point marked as PP in Fig. 4.4 corresponds to the plait point of the mixture calculated according to the graphical approach proposed by Treybal *et. al.* (Treybal *et al.,* 1946; Treybal, 1963(a)). Fig. 4.5 shows the result of the consistency analysis of the measured phase compositions using the methods by Hand (Hand, 1929), Bachman (Bachman, 1940), and Othmer-Tobias (Othmer and Tobias, 1942) described in Section 3.4.2. The measured phase compositions presented in Fig. 4.5 agree with the fitted L_1L_2 boundaries within the error of the measurement. The results of the consistency check shown in Fig. 4.5 indicate that measured phase compositions at 0, 21, 50, and 70°C are thermodynamically consistent as they produced straight lines as required by methods by Hand (Hand, 1929), Bachman (Bachman, 1940), and Othmer-Tobias (Othmer and Tobias, 1942). All the data collected as well as the calculated plait points are summarized in the Appendix B.

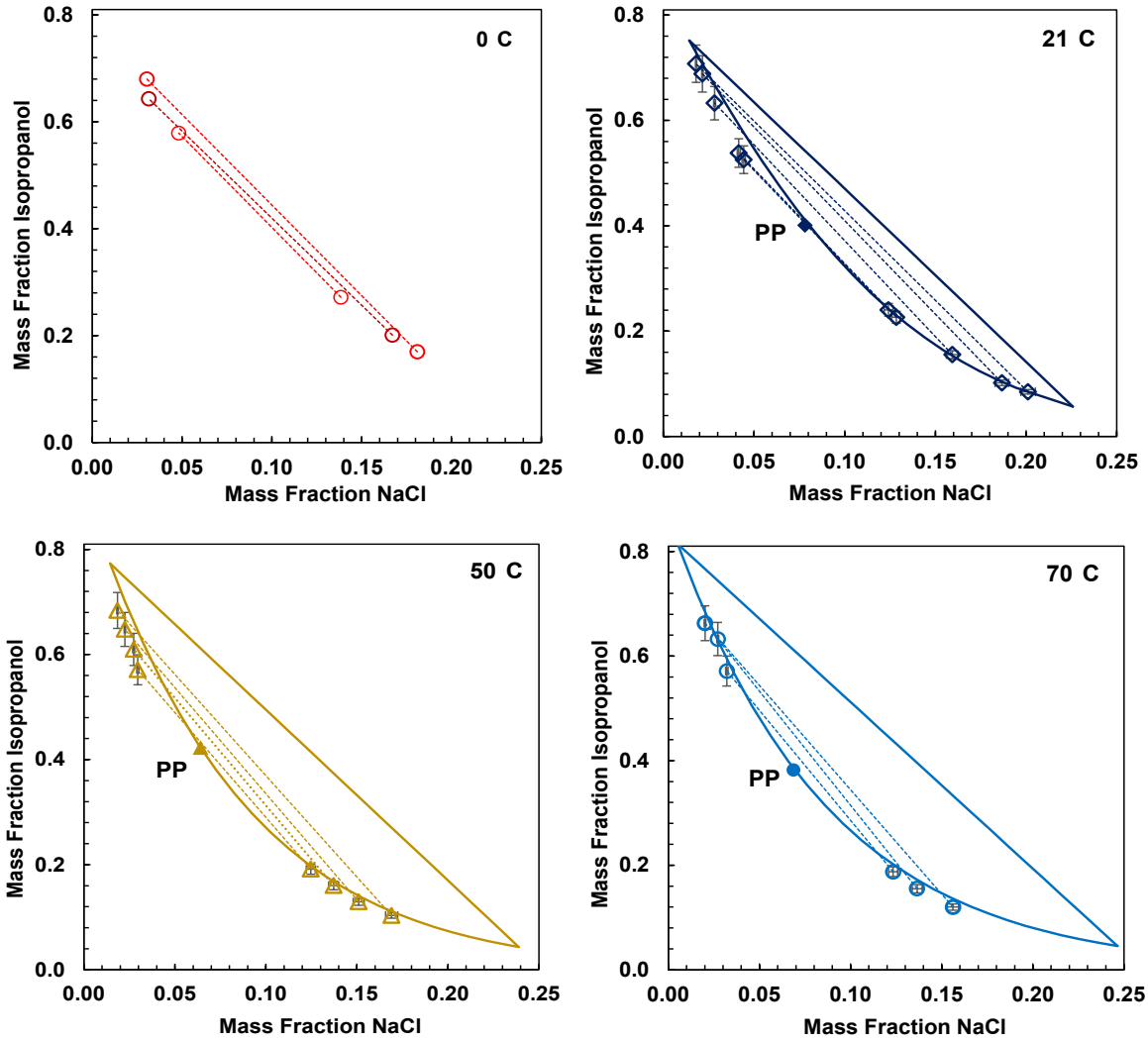

Figure 4.4. Plotted liquid-liquid equilibrium phase composition data at 0, 21, 50, and 70˚C and atmospheric pressure. The dashed lines are the tie lines, and PP shows the plait point. Solid lines are the L_1L_2 and L_1L_2S phase boundaries.

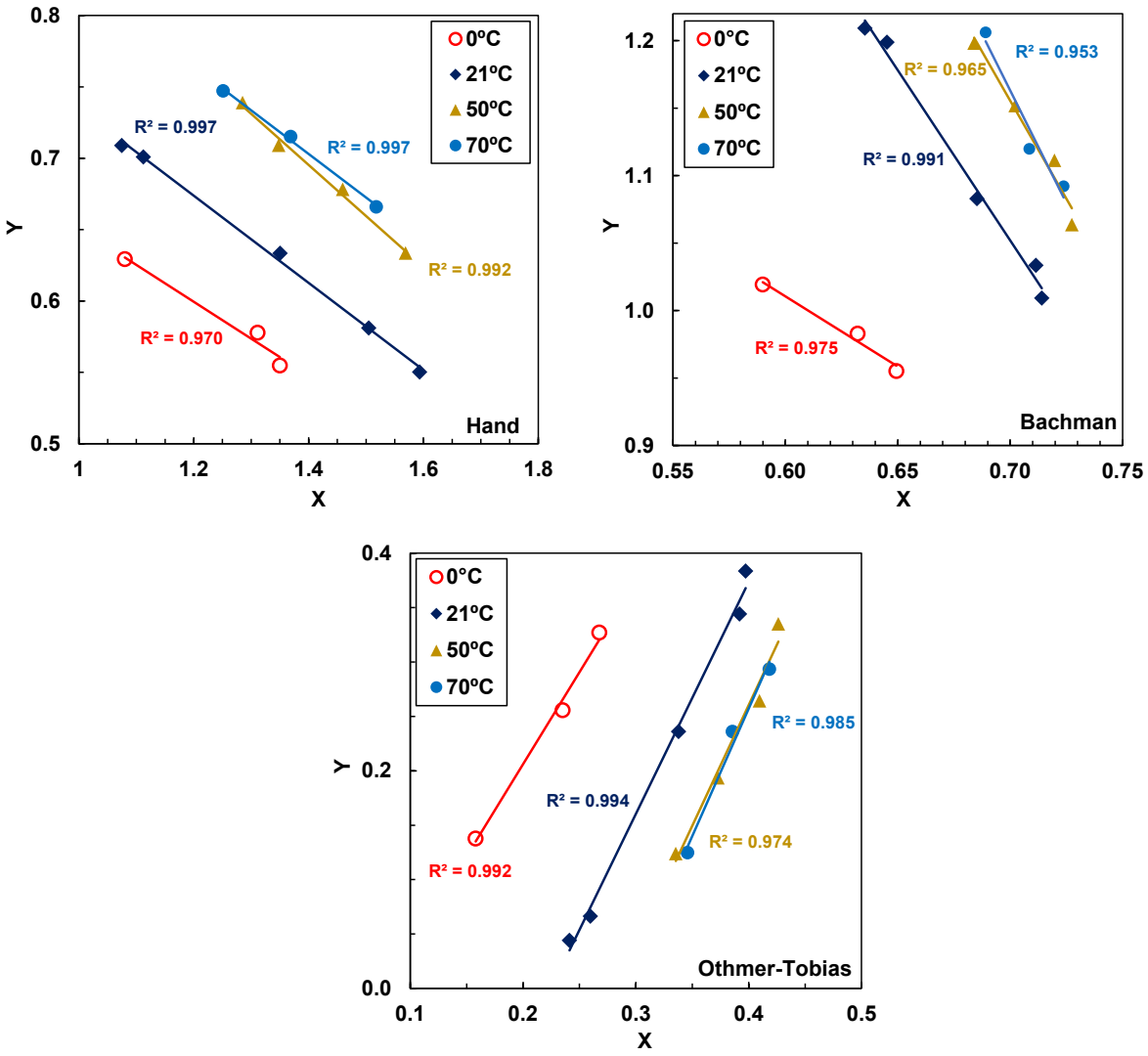

Figure 4.5. The thermodynamic consistency check for the liquid-liquid equilibrium phase composition data at 0, 21, 50, and 70˚C and atmospheric pressure. The symbols are resulted by the equations described in Table 3.1. The solid straight lines show the consistency of the data based on three methods.

Fig. 4.5 also provides information on the effect of temperature on phase compositions because the parameters X and Y are dependent on measured phase compositions. Phase compositions are sensitive to temperatures between 0 and 50°C; however, when comparing the trends at 50 and 70°C, there is not a significant difference between them indicating that phase compositions at these two temperatures are similar. This result is not surprising as the area of the liquid-liquid envelope did not change significantly from 50 to 70°C as previously discussed.

The slope of the tie-line (STL) can be used to assess the effect of temperature on the composition of the isopropanol-rich, or organic, phase. This parameter is defined as follows (Khayati and Gholitabar, 2016; Zafarani-Moattar *et al.,* 2019; Pimentel *et al.,* 2017):

$$STL = \frac{wt_{isopropanol}^{Organic} - wt_{isopropanol}^{Aqueous}}{wt_{NaCl}^{Organic} - wt_{NaCl}^{Aqueous}} \quad (4.3)$$

Eq. 4.3 was used for the calculation of the slope of the tie-lines shown in Fig. 4.4. The averaged STL values at 0, 21, 50, and 70°C are presented in Fig. 4.5. The error bars indicate the range of the STL values at each temperature. In general, the absolute values of STL increase with temperature indicating the organic phase becomes richer in isopropanol. However, when comparing the STL values at 50 and 70°C, the error bars overlap suggesting there is not a significant difference in the isopropanol contents at these two temperatures as previously stated.

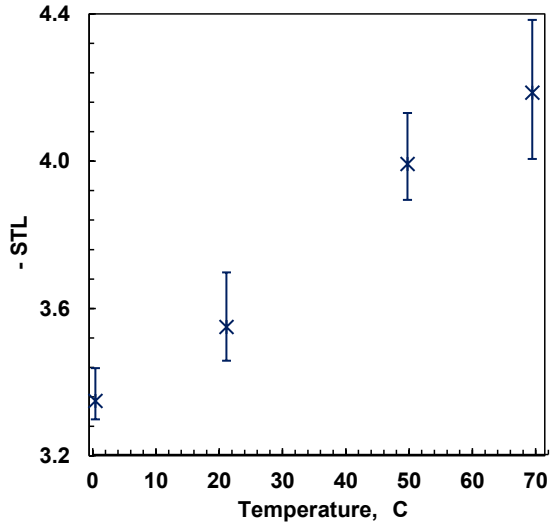

Figure 4.6. The ranges of the STL for the liquid-liquid equilibrium phase composition data at 0, 21, 50, and 70˚C and atmospheric pressure.

4.4 Vapor-Liquid Equilibrium

The measured normal boiling points and the liquid and vapor phase compositions (in mass fraction) for isopropanol/water/NaCl mixtures are shown in Fig. 4.7 panels a and b, respectively. The variable in abscissa corresponds to the mass fraction of isopropanol in the solvent defined as a liquid mixture of isopropanol and water. The solid lines included in Fig. 4.7 a and b correspond to predicted normal boiling points and phase compositions, respectively, from the electrolyte version of the UNIQUAC model with the parameters reported by Thomsen (Thomsen, 1997(a)). For comparison purposes, measured and predicted (dashed lines) normal boiling points and phase

compositions for isopropanol/water mixtures were also included in Fig. 4.7 a and b. All the measured data shown in Fig. 4.7 was collected at isopropanol content in the solvent below the vapor-liquid-liquid (VL_1L_2) boundary, *i.e.*, in the region where only a single liquid phase exists at equilibrium with the vapor phase (VL region). The predicted data were calculated at isopropanol content in the solvent up to approximately the VL_1L_2 boundary. This boundary was visually detected experimentally; however, the experimental methodology was not accurate enough for the determination of temperatures and phase compositions at the VL_1L_2 boundary. For mixtures with NaCl mass content of 5 wt%, the electrolyte version of the UNIQUAC model detected the VL_1L_2 boundary at isopropanol mass fraction in the solvent equal to 0.45 whereas this boundary was visually detected approximately at isopropanol mass fraction in the solvent of 0.50. The electrolyte version of the UNIQUAC model predicted the normal boiling points and phase compositions with AARD of 5% and 9%, respectively. The maximum deviations were found at a salt mass content of 20 wt%.

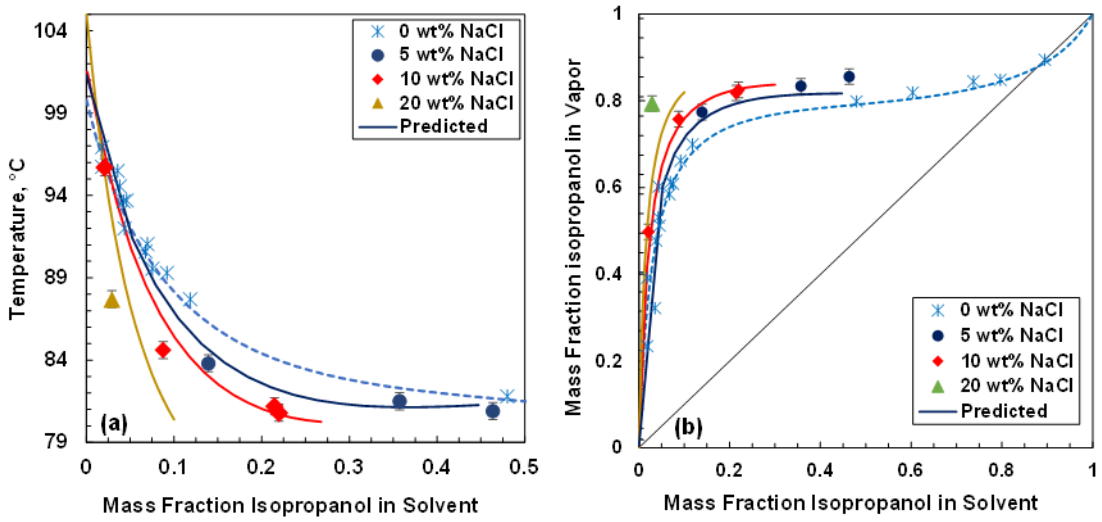

Figure 4.7. (a) VLE compositions of isopropanol in the solvent at different salt concentrations for isopropanol/water/NaCl mixture. (b) Compositions of isopropanol in the vapor phase and the salt-free liquid phase for the VLE of isopropanol/water/NaCl mixture. All data was collected at atmospheric pressure. Dashed lines are the composition data for the VLE of the isopropanol/water mixture. Solid lines were predicted by the E-UNIQUAC model.

In general, the normal boiling point temperature of isopropanol/water/NaCl mixtures decreases as the salt mass content increases. At constant NaCl mass content, the highest normal boiling point corresponds to that of a saturated solution of NaCl in pure water and rapidly decreases as the

isopropanol content in the solvent increases until it reaches the lowest value at the VL_1L_2 boundary, Fig. 4.7a. As the mass content of NaCl increases, the mixture becomes more unstable and the VL_1L_2 boundary is reached at lower isopropanol mass content in the solvent. This rapid decrease in the normal boiling point temperature as the NaCl content increases indicates that the volatile isopropanol is being rejected from the liquid phase and into the vapor phase. This argument is supported by the data presented in Fig. 4.7b which indicates the vapor phase becomes richer in isopropanol as the NaCl mass content in the liquid mixture increases.

4.5 Qualitative Comparison Between Salting-Out and Heterogenous Azeotropic Distillation for Producing High Purity Isopropanol

As discussed in Chapter 1, isopropanol is industrially produced through direct or indirect hydration of propylene in a catalytic reactor. The product leaving the reactor contains, approximately, 70wt% water, 25 wt% isopropanol and 5 wt% diisopropyl ether. The isopropanol is separated off this product stream by heterogenous azeotropic distillation to produce a final product with an isopropanol purity of 99 wt% (Chua *et al.*, 2017). This complex distillation technology is required as isopropanol forms a low normal boiling point binary azeotrope with water at an isopropanol mass content of 87.4 wt%. In heterogeneous azeotropic distillation, cyclohexane is added to the condenser of the first distillation column to form a heterogeneous azeotrope with the isopropanol/water mixture. The top stream of the first distillation tower is rich in water and cyclohexane with an isopropanol content above 20 wt%; and the bottom stream is the desired product (99 wt% isopropanol), Fig. 4.8. The top product from the first distillation tower is condensed into two liquid phases: one rich in cyclohexane and the other rich in isopropanol and water. The cyclohexane-rich phase is refluxed into the first column and the liquid phase rich in isopropanol and water is sent to a second distillation column needed to recover as much of the isopropanol as possible. The top product from the second distillation column is a mixture of isopropanol/water/cyclohexane at the ternary azeotropic composition and the bottom product is a mixture of isopropanol/water with isopropanol content below the binary azeotropic composition. This bottom product is fed into a third distillation tower that produces a mixture of isopropanol and water at the azeotropic composition through the top and wastewater through the bottom. The top product of the third distillation tower is recycled back to the first distillation tower, Fig. 4.8.

Heterogeneous azeotropic distillation is costly and the columns are difficult to operate and control (Arifin *et al.,* 2007; Chien *et al.,* 2004; Chang *et al.,* 2012).

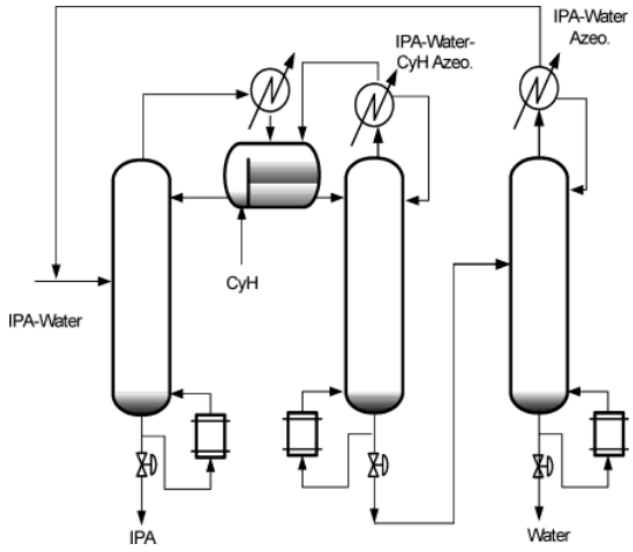

Figure 4.8 Flowsheet of the three-column system required for the heterogenous azeotropic distillation of isopropanol/water mixtures. IPA and CyH stand for isopropanol and cyclohexane, respectively. Figure adapted from Chien *et al*. (Chien *et al.,* 2004).

The salting-out purification method studied here does not produce high purity isopropanol as that obtained from heterogenous azeotropic distillation. The maximum isopropanol purity produced from salting-out was 83 wt%. Therefore, to increase the purity of the final product, additional distillation steps may be needed and consequently experimental data from the liquid-liquid-vapor and liquid-liquid-solid-vapor regions of the phase diagram are required.

Chapter 5: Conclusions and Recommendations

5.1 Conclusions

The liquid-solid, liquid-liquid, liquid-liquid-solid, and liquid-vapor regions of the phase diagram of the mixture isopropanol/water/NaCl were mapped at atmospheric pressure using experimental procedures tested and validated in this study. The effect of the temperature on the solid-liquid, liquid-liquid, and liquid-liquid-solid phase boundaries was studied from room temperature to 70°C. Liquid-liquid phase compositions were experimentally measured from 0 to 70°C; the thermodynamic consistency of the measured compositions was checked using the graphic methods proposed by Hand (Hand, 1929), Bachman (Bachman, 1940), and Other and Tobias (Othmer and Tobias, 1942); and the corresponding plait points were calculated according to the method proposed by Treybal (Treybal, 1963(a)). The effect of NaCl mass content in the normal boiling point temperatures of the mixtures was measured and the corresponding compositions of the liquid and vapor phases were also measured.

Two liquid-solid regions were detected. In one of these, the liquid was rich in water (termed L_1S) and in the other, the liquid was rich in isopropanol (termed L_2S). The location of the boundary between the L_1S and the single liquid (L) regions was slightly affected by the temperature whereas that between the L_2S and L regions was not significantly affected by the temperature. This result is consistent with the slight increase in the solubility of NaCl in water with the temperature and the no solubility of NaCl in isopropanol, respectively. The boundaries between the two-liquid phase (termed L_1L_2) and the single liquid (L) phase regions were affected as the temperature was increased from room to 50°C; however, this boundary was not significantly affected as the temperature was increased from 50 to 70°C. Similar results were obtained for the boundary between the L_1L_2 and the liquid-liquid-solid (L_1L_2S) regions.

All the measured liquid-liquid phase compositions passed the thermodynamic consistency checks established by the graphical methods proposed by Hand (Hand, 1929), Bachman (Bachman, 1940), and Other and Tobias (Othmer and Tobias, 1942). For all these three checks, the measured compositions produced straight lines as required by these methods to ensure thermodynamic consistency. The magnitude of the slope of the measured tie lines (STL) was used to assess the

effect of the temperature on the compositions of the two liquid phases: the higher the magnitude of the STL the higher the isopropanol content in the isopropanol-rich, or organic, phase. The results of this analysis indicated that as the temperature increased from 0 to 50°C the magnitude of the STL increased indicating more isopropanol in the isopropanol-rich phase. However, when comparing the calculated STL at 50 and 70°C, there was not a significant difference between these two values indicating that the temperature does not have a significant effect on the isopropanol mass content in the isopropanol-rich phase in this temperature range.

The measured vapor-liquid equilibrium data showed that normal boiling points and vapor-liquid phase compositions are affected by the NaCl mass content in the mixture. At constant NaCl mass content, the normal boiling point of the mixture decreases rapidly as the mass fraction of isopropanol in the solvent increases. The solvent is the isopropanol/water liquid blend used to dissolve the NaCl. The maximum and the minimum boiling points correspond to that of pure water saturated with NaCl and that at the boundary between the vapor-liquid and the vapor-liquid-liquid regions. At constant isopropanol mass fraction in the solvent, the normal boiling point of the mixture decreases as the NaCl mass content increases. These results indicate that the presence of NaCl in the mixture reduces the affinity of water and isopropanol increasing the relative volatility of the isopropanol causing it to split into the vapor phase. This observation was corroborated by the measured composition of the vapor phase which becomes richer in isopropanol at higher NaCl mass content in the liquid.

5.2 Recommendations

1. The boiling point of isopropanol at atmospheric pressure (82.5°C) limits the application of the experimental procedures presented in this study for the determination of liquid-solid, liquid-liquid, and liquid-liquid-solid phase boundaries. It was found that at temperatures above 72°C, isopropanol starts boiling which makes the data collection very challenging. It is recommended to design a high-pressure equilibrium cell to avoid this issue.

2. In order to map the entire phase diagram for the isopropanol/water/NaCl mixture, the phase boundary between VL and VLL regions should be determined. However, by the experimental apparatus used in this research, the determination of this boundary is quite

challenging. Therefore, the experimental data for the VLL phase boundary should be obtained with a developed experimental setup.

References

Al-Abdullah, M. H., G. T. Kalghatgi, and H. Babiker. 2015. "Flash Points and Volatility Characteristics of Gasoline/Diesel Blends." Fuel 153 (August): 67–69.

Amidonx, G. L., S. H. Yalkowsky, and S. Leung. 1974. "Solubility of Nonelectrolytes in Polar Solvents 11: Solubility of Aliphatic Alcohols in Water." *Journal of Pharmaceutical Sciences* 63: 1858–66.

Andersen, V. F., J. E. Anderson, T. J. Wallington, S. A. Mueller, and O. J. Nielsen. 2010. "Vapor Pressures of Alcohol-Gasoline Blends." *Energy and Fuels* 24 (6): 3647–54.

Arifin, Saiful, and I-Lung Chien. 2007. "Combined Preconcentrator/Recovery Column Design for Isopropyl Alcohol Dehydration Process." Ind. Eng. Chem. Res. 46 (8): 2535–43.

Arifin, Yalun, Ellen Tanudjaja, Arbi Dimyati, and Reinhard Pinontoan. 2014. "A Second Generation Biofuel from Cellulosic Agricultural By-Product Fermentation Using Clostridium Species for Electricity Generation." *Energy Procedia* 47: 310–15.

Arzideh, Seyyed Mohammad, Kamyar Movagharnejad, and Mohsen Pirdashti. 2018. "Influence of the Temperature, Type of Salt, and Alcohol on Phase Diagrams of 2-Propanol + Inorganic Salt Aqueous Two-Phase Systems: Experimental Determination and Correlation." *J. Chem. Eng. Data* 63 (8): 2813–24.

Atsumi, Shota, Taizo Hanai, and James C Liao. 2008. "Non-Fermentative Pathways for Synthesis of Branched-Chain Higher Alcohols as Biofuels." *Nature* 451: 86–89.

Bachman, Irvin. 1940. "Tie Lines in Ternary Liquid Systems" 13: 38–39.

Bharmoria, Pankaj, Hariom Gupta, V. P. Mohandas, Pushpito K. Ghosh, and Arvind Kumar. 2012. "Temperature Invariance of NaCl Solubility in Water: Inferences from Salt−Water Cluster Behavior of NaCl, KCl, and NH(4)Cl." *J. Phys. Chem. B* 116: 34.

Briscoe, B., P. Luckham, and S. Zhu. 2000. "The Effects of Hydrogen Bonding upon the Viscosity of Aqueous Poly(Vinyl Alcohol) Solutions." *Polym. J.* 41 (10): 3851–60.

Brownstein, M. 2015. *Renewable Motor Fuels The Past: The Present and the Uncertain Future*.

Sivasubramanian, Pochareddy Y. K., Dhamodaran G., Esakkimuthu G. S., 2017. "Performance, emission and combustion characteristics of a branched higher mass, C3 alcohol (isopropanol) blends fuelled medium duty MPFI SI engine" *Eng. Saci. Technol. Int. J.* 20: 528–535.

Cantero, Carlos Alberto Torres, Guadalupe Lopez Lopez, Victor M. Alvarado, Ricardo F. Escobar Jimenez, Jesse Y.Rumbo Morales, and Eduardo M.Sanchez Coronado. 2017. "Control Structures Evaluation for a Salt Extractive Distillation Pilot Plant: Application to Bio-Ethanol Dehydration." *Energies* 10 (9): 1276.

Chang, Wen-Teng, Chi-Tsung Huang, and Shueh-Hen Cheng. 2012. "Design and Control of a Complete Azeotropic Distillation System Incorporating Stripping Columns for Isopropyl Alcohol Dehydration." Ind. Eng. Chem. Res. 51: 2997–3006.

Chien, I-Lung, Kai-Luen Zeng, and Huan-Yi Chao. 2004. “Design and Control of a Complete Heterogeneous Azeotropic Distillation Column System.” Ind. Eng. Chem. Res. 43 (9): 2160–74.

Chou, Tzu Jen, Akihiko Tanioka, and Hsieng Cheng Tseng. 1998. “Salting Effect on the Liquid−Liquid Equilibria for the Partially Miscible Systems of N-Propanol−Water and i-Propanol−Water.” Industrial and Engineering Chemistry Research 37 (5): 2039–44.

Chua, W. J., G. P. Rangaiah, and K. Hidajat. 2017. “Design and Optimization of Isopropanol Process Based on Two Alternatives for Reactive Distillation.” Chemical Engineering and Processing: Process Intensification 118: 108–16.

Carlo Edgar, Torres Ortegaa, and BenGuang Rong. 2016. “Intensified Separation Processes for the Recovery and Dehydration of Bioethanol from an Actual Lignocellulosic Fermentation Broth.” *Computer Aided Chemical Engineering* 38: 727–32.

Demenezes, E., R. Cataluna, D. Samios, and R. Silva. 2006. “Addition of an Azeotropic ETBE/Ethanol Mixture in Eurosuper-Type Gasolines.” *Fuel* 85 (17–18): 2567–77.

Eisen, Edwin O., and Joseph Joffe. 1966. “Salt Effects in Liquid-Liquid Equilibria.” *J. Chem. Eng. Data* 4: 480–84.

EPA Agency. 2020. “Sources of Greenhouse Gas Emissions.” https://www.epa.gov/ghgemissions/sources-greenhouse-gas-emissions.

Frankforter, G. B., and F. C. Frary. 1913. “Equilibria in Systems Containing Alcohols, Salts and Water.” *J. Phys. Chem.* 17 (402).

Fuentes-Azcatl, Raúl, and Marcia C. Barbosa. 2016. “Sodium Chloride, NaCl/∈: New Force Field.” *Journal of Physical Chemistry B* 120 (9): 2460–70.

Gironi, F., and L. Lamberti. 1995. “Vapor-Liquid Equilibrium Data for the Water-2-Propanol System in the Presence of Dissolved Salts.” *Fluid Phase Equilibria* 105 (2): 273–86.

Gomis, Alejandro, Jorge Garcia-Cano, Juan Carlos Asensi, and Vicente Gomis. 2018. “Equilibrium Diagrams of Water + NaCl or KCl + 2-Methyl 2-Propanol at the Boiling Temperature and 101.3 KPa.” *Journal of Chemical and Engineering Data* 63 (11): 4107–13.

Gomis(a), Vicente, Francisco Ruiz, Guillermo De Vera, Eladio Lbpez, and M Dolores Saquete. 1994. “Liquid-Liquid-Solid Equilibria for the Ternary Systems Water-Sodium Chloride or Potassium Chloride-1-Propanol or 2-Propanol.” *Fluid Phase Equilibria* 98: 141–47.

Guo, Senqi, Chun Zhu, Guoqing Chen, Jiao Gu, Chaoqun Ma, Hui Gao, Lei Li, *et al.* 2022. “A Theoretical Study on Intermolecular Hydrogen Bonds of Isopropanol-Water Clusters.” *Theoretical Chemistry Accounts* 141 (1).

Hand, David Birney. 1929. “The Distribution of a Consolute Liquid between Two Immiscible Liquid.”

Hartanto, Dhoni, Prima Astuti Handayani, Akhmad Sutrisno, Viona Widya Anugrahani, Asalil Mustain, and Ianatul Khoiroh. 2019. “Isopropyl Alcohol Purification through Extractive

Distillation Using Glycerol as an Entrainer: Technical Performances Simulation and Design." *Jurnal Bahan Alam Terbarukan* 8 (2): 133–43.

Hu, Mancheng, Xiang Zhu, ni Li, Quanguo Zhai, Yucheng Jiang, Xiaoyan Lin, and Chengshan Tuo. 2009. "Liquid-Liquid Equilibria for Methanol/Ethanol + Rubidium Carbonate + Water Systems at Different Temperatures Liquid-Liquid Equilibria for the Two Ternary Systems of CH." *J. Chem. Eng. Data* 54 (10): 2866–70.

Ignatov, Ignat, Fabio Huether, Nikolai Neshev, Yoana Kiselova-Kaneva, Teodora P. Popova, Ralitsa Bankova, Nedyalka Valcheva, *et al.* 2022. "Research of Water Molecules Cluster Structuring during Haberlea Rhodopensis Friv. Hydration." *Plants* 11 (19): 2655.

International Energy Agency. 2022. "Biofuels." 2022. https://www.iea.org/reports/biofuels.

Karimi, Samira, Rama Rao Karri, Mohammad Tavakkoli Yaraki, and Janardhan Reddy Koduru. 2021. "Processes and Separation Technologies for the Production of Fuel-Grade Bioethanol: A Review." *Environmental Chemistry Letters* 19 (4): 2873–90.

Katayama, Hirotake, and Masahito Miyahara. 2006. "Liquid-Liquid Phase Equilibria of (Ethanol or Methanol + Water) Containing Either Dipotassium Hydrogen Phosphate or Sodium Dihydrogen Phosphate." *J. Chem. Eng. Data* 51: 914–18.

Khayati, Gholam, and Amir Gholitabar. 2016. "Liquid-Liquid Equilibrium of Hydrophilic Alcohols with Three Different Salts of Chloride: Experiment and Correlation." *Journal of Chemical and Engineering Data* 61 (4): 1454–61.

Khayati, Gholam, Siamak Ashraf Talesh, and Mandana Yazdanshenas. 2014. "Partitioning of Propionic Acid in Polyethylene Glycol/ Different Salts of Sulfate Aqueous Two-Phase Systems." *Separation Science and Technology (Philadelphia)* 49 (17): 2741–47.

Kirn, E. R., and H. L Dunlap. 1931. "The Solubilities of Alkali Chlorides and Sulfates in Anhydrous Alcohols." *J. Am. Chem. Soc.* 53 (2): 391–94.

Ko, Young Jin, Joy Cha, Wu Young Jeong, Myeong Eun Lee, Byeong Hyeon Cho, Bhardwaj Nisha, Hyun Jin Jeong, Sung Eun Park, and Sung Ok Han. 2022. "Bio-Isopropanol Production in Corynebacterium Glutamicum: Metabolic Redesign of Synthetic Bypasses and Two-Stage Fermentation with Gas Stripping." *Bioresour.. Technol.* 354 (June).

Koppolu, Veerendra, and Veneela KR Vasigala. 2016. "Role of Escherichia Coli in Biofuel Production." *Microbiology Insights* 9 (January): 29–35.

Kroschwitz, J. I. 1991. *Kirk–Othmer Encyclopedia of Chemical Technology, 4th Edition*. 4th ed. Vol. 20. , New York, USA.

Kunwer, Ram, S. R. Pasupuleti, S. S. Bhurat, S. K Gugulothu, and N. Rathore. 2022. "Blending of Ethanol with Gasoline and Diesel Fuel – a Review." *Mater Today* 69 (January): 560–63.

Larsen, R. G., and Hunt Herschel. 1939. "Molecular Forces and Solvent Power." *J. Phys. Chem.* 43 (4): 417–23.

Lebo, Robert B. 1921. “Properties of Mixtures of Isopropyl Alcohol and Water.” Journal of the American Chemical Society 43 (5): 1005–11.

Lin, Yan, and Shuzo Tanaka. 2006. “Ethanol Fermentation from Biomass Resources: Current State and Prospects.” *Applied Microbiology and Biotechnology* 69 (6): 627–42.

Malmberg, C G, and A A Maryott. 1956. “Dielectric Constant of Water from 0 0 to 100 0 C.” *Journal of Research of the National Bureau of Standards*. Vol. 56.

Marcus, Yizhak. 1991. “Thermodynamics of Solvation of Ions Part 5, Gibbs Free Energy of Hydration at 298.15 K.” *J. Chem. SOC., Faraday Trans* 87 (18): 2995–99.

Martins, João Paulo, Jane S. Dos Reis Coimbra, Fabíola Cristina De Oliveira, Guilherme Sanaiotti, César A.S. Da Silva, Luis Henrique Mendes Da Silva, and Maria Do Carmo H. Da Silva. 2010. “Liquid-Liquid Equilibrium of Aqueous Two-Phase System Composed of Poly(Ethylene Glycol) 400 and Sulfate Salts.” *Journal of Chemical and Engineering Data* 55 (3): 1247–51.

Merchuk, Jose C, Barbara A Andrews, and Juan A Asenjo. 1998. “Aqueous Two-Phase Systems for Protein Separation Studies on Phase Inversion.” *Journal of Chromatography B* 711: 285–93.

Miller C. G., and Maass O. 1960. “Determination of Dielectric Constant in Binary Organic Systems.” *Can. J. Chem* 38.

Morrison, J F, J C Baker, H C Meredith III, K E Newman, T D Walter, J D Massle, R L Perry, and P T Cummings. 1990. “Experimental Measurement of Vapor-Liquid Equilibrium in Alcohol/Water/Salt Systems.” *Ind. Eng. Chem* 35 (10): 259.

Muniz, Izabella de Carvalho Batista, Sérgio de Sousa Castro, Olga Reinert Ramos Gandolfi, Karine Amaral dos Santos, Beatriz Silva Santos, Evaldo Cardozo Souza Junior, Rafael da Costa Ilhéu Fontan, Cristiane Martins Veloso, and Renata Cristina Ferreira Bonomo. 2021. “Liquid-Liquid Equilibrium Data for Systems Formed by Peg (4000 Or 6000) or Alcohol (1-Propanol or 2-Propanol) + Potassium Phosphate + Water: Experimental Measurements, Correlations and Thermodynamic Modeling.” *J. Mol. Liq* 343 (December).

Nemati-Kande, Ebrahim, and Hemayat Shekaari. 2013. “Thermodynamic Investigation of the ATPSs Composed of Some (Aliphatic Alcohol + Sodium Carbonate + Water) Ternary Systems.” *J. Chem. Thermodyn* 57 (February): 541–49.

Nemati-Kande, Ebrahim, Hemayat Shekaari, and Mohammed Taghi Zafarani-Moattar. 2012. “Binodal Curves and Tie-Lines of Aliphatic Alcohols + Diammonium Hydrogen Citrate + Water Ternary Systems: Measurement and Modeling.” *J. Chem. Eng. Data* 57: 16.

National Institute of Standard and Technology (NIST). 2008. “Standard Reference Database, WinSource.” Gaithersburge, MD.

Ohe, Shuzo. 1998. “Prediction of Salt Effect on Vapor-Liquid Equilibria.” *Fluid Phase Equilibria* 144 (1–2): 119–29.

Othmer, Donald F, and Philip E Tobias. 1942. “TIE LINE CORRELATION.” Vol. 13. UTC.

Palit, Santis R. 1947. “Electronic Interpretations of Organic Chemistry. It Interpretation of the Solubility of Organic Compounds.” *J Phys Colloid Chem* 837: 51.

Panjapakkul, Warissara, and Mahmoud M. El-Halwagi. 2018. “Technoeconomic Analysis of Alternative Pathways of Isopropanol Production.” *ACS Sustainable Chemistry and Engineering* 6 (8): 10260–72.

Pimentel, Juliana Gomes, Silvana Ferreira Bicalho, Olga Reinert Ramos Gandolfi, Lizzy Ayra Alcântara Verissimo, Sérgio de Sousa Castro, Erik Almeida Souza, Cristiane Martins Veloso, Rafael da Costa Ilhéu Fontan, Vanessa Santos Sampaio, and Renata Cristina Ferreira Bonomo. 2017. “Evaluation f Salting-Out Effect in the Liquid–Liquid Equilibrium of Aqueous Two-Phase Systems Composed of 2-Propanol and Na2SO4/Mgso4 at Different Temperatures.” *Fluid Phase Equilibria* 450 (October): 184–93.

Pinho, Simão P., and Eugénia A. Macedo. 2005. “Solubility of NaCl, NaBr, and KCl in Water, Methanol, Ethanol, and Their Mixed Solvents.” *Journal of Chemical and Engineering Data* 50 (1): 29–32.

Pirdashti, Mohsen, Kamyar Movagharnejad, Abbas Ali Rostami, Pegah Akbarpour, and Mahnam Ketabi. 2015. “Liquid-Liquid Equilibrium Data, Viscosities, Densities, Conductivities, and Refractive Indexes of Aqueous Mixtures of Poly(Ethylene Glycol) with Trisodium Citrate at Different PH.” *Journal of Chemical and Engineering Data* 60 (11): 3423–29.

Polka, Hans-Martin, and Jürgen Gmehling. 1994. “Effect of Calcium Nitrate on the Vapor-Liquid Equilibria of Ethanol + Water and 2-Propanol + Water.” *J. Chem. Eng. Data* 39: 621–24.

Prausnitz, John M., Rudiger N. Lichtenthaler, and Edmundo Gomes de Azevedo. 1978. *Molecular Thermodynamics of Fluid Phase Equilibria 3Ed*.

Ramos-Pallares, F. 2023. “Personal Communication Reference, Lakehead University.”

Reber, L A, W M Mcnabb, and W W Lucasse. 1941. “The Effect of Salts on the Mutual Miscibility of Normal Butyl Alcohol and Water.” Philadelphia.

Rochón, Eloísa, Florencia Cebreiros, Mario Daniel Ferrari, and Claudia Lareo. 2019. “Isopropanol-Butanol Production from Sugarcane and Sugarcane-Sweet Sorghum Juices by Clostridium Beijerinckii DSM 6423.” *Biomass and Bioenergy* 128 (September): 105331.

Rogers, James W, Jack W Knight, and A R Choppin. 1947. “An Improved Apparatus for Determining Vapor-Liquid Equilibrium.”

Rongqi, Zhou, and Duan Zhanting. 1999. “Extractive Distillation with Salt in Solvent.” *Tsinghua Sci Technol* 4 (2).

Salabat, Alireza, and Mahmod Hashemi. 2006. “Temperature Effect on the Liquid-Liquid Equilibria for Some Aliphatic Alcohols + Water + K(2)CO(3)Systems.” *J. Chem. Eng. Data* 51 (4): 1194–97.

Santis, R De, L Marrelli, and P N Muscetta. 1976. “Liquid-Liquid Equilibria in Water-Aliphatic Alcohol Systems in the Presence of Sodium Chloride.” *The Chemical Engineering Journal, 1 I*, 207–14.

Schmitt, D. 1979. “Ph. D. Thesis.” University of Karlsruhe, Germany.

Silva, Luís H.M. Da, and Watson Loh. 2000. “Calorimetric Investigation of the Formation of Aqueous Two-Phase Systems in Ternary Mixtures of Water, Poly(Ethylene Oxide) and Electrolytes (or Dextran).” *Journal of Physical Chemistry B* 104 (43): 10069–73.

Silva(a), Rosângela Da, Renato Cataluña, Eliana Weber De Menezes, Dimitrios Samios, and Clarisse M.Sartori Piatnicki. 2005. “Effect of Additives on the Antiknock Properties and Reid Vapor Pressure of Gasoline.” *Fuel* 84 (7–8): 951–59.

Slaughter, R. J., R. W. Mason, D. M.G. Beasley, J. A. Vale, and L. J. Schep. 2014. “Isopropanol Poisoning.” *Clinical Toxicology* 52 (5): 470–78.

Smith, J. M. (Joseph Mauk), H. C. (Hendrick C.) Van Ness, Michael M. Abbott, and Mark T. (Mark Thomas) Swihart. 1965. *Introduction to Chemical Engineering Thermodynamics*.

Sretenskaja, N G, Richard J Sadus, and E Ulrich Franck. 1995. “High-Pressure Phase Equilibria and Critical Curve of the Water + Helium System to 200 MPa and 723 K+.” *J. Phys. Chem*. Vol. 99.

Survase, Shrikant A, German Jurgens, Adriaan Van Heiningen, and Tom Granström. 2011. “Continuous Production of Isopropanol and Butanol Using Clostridium Beijerinckii DSM 6423.” *Appl. Microbiol. Biotechnol.* 91: 1305–13.

Thomsen, Kaj. 2009. *General Rights Electrolyte Solutions: Thermodynamics, Crystallization, Separation Methods*.

Thomsen(a), Kaj. 1997. “Aqueous Electrolytes Model Parameters and Process Simulation.” *Citation*. Lyngby, Denmark: Technical University of Denmark.

Treybal, Treybal, Robert E, Lawrence D. Weber, and Joseph F. Daley. 1946. “The System Acetone-Water-1,1,2-Trichloroethane.” *J Ind Eng Chem* 38: 817–21.

Treybal(a), Robert E. 1963. *Liquide Extraction*. 2nd ed. New York: Mc Graw-Hill.

US Department of Energy. 2022. “Global Ethanol Production by Country or Region.” 2022. https://afdc.energy.gov/data.

Vercher, E, R Muñoz, and A Mart Inez-Andreu. 1991. “Isobaric Vapor-Liquid Equilibrium Data for the Ethanol-Water-Potassium Acetate and Ethanol-Water-(Potassium Acetate/Sodium Acetate) Systems.” *J. J. Chem. Eng. Data* 36 (16): 277–80.

Xu, Li, Dongmei Xu, Puyun Shi, Kai Zhang, Xiaolong Ma, Jun Gao, and Yinglong Wang. 2018. “Salts Effect on Isobaric Vapor−Liquid Equilibrium for Separation of the Azeotropic Mixture Allyl Alcohol + Water.” *Fluid Phase Equilibria* 457 (February): 11–17.

Xu, Y., K. T. Chuang, and A. R. Sanger. 2002. “Design of a Process for Production of Isopropyl Alcohol by Hydration of Propylene in a Catalytic Distillation Column.” *Chemical Engineering Research and Design* 80 (6): 686–94.

Yarranton, H. W., J. C. Okafor, D. P. Ortiz, and F. G.A. Van Den Berg. 2015. “Density and Refractive Index of Petroleum, Cuts, and Mixtures.” *Energy and Fuels* 29 (9): 5723–36.

Zafarani-Moattar, Mohammed Taghi, and Parisa Jafari. 2013. “The Effect of Temperature on the Liquid-Liquid Equilibria of Some Aliphatic Alcohols+Di-Sodium Hydrogen Citrate+Water Systems: Experimental and Correlation.” *Fluid Phase Equilibria* 353 (September): 50–60.

Zafarani-Moattar, Mohammed Taghi, Hemayat Shekaari, and Parisa Jafari. 2019. “Liquid-Liquid Equilibria of Choline Chloride + 1-Propanol or 2-Propanol + Water Ternary Systems at Different Temperatures: Study of Choline Chloride Ability for Recovering of These Alcohols from Water Mixtures.” *Journal of Molecular Liquids* 273 (January): 463–75.

APPENDIX A:

EXPERIMENTALLY MEASURED LIQUID-SOLID, LIQUID-LIQUID AND LIQUID-LIQUID-SOLID PHASE BOUNDARIES FOR ISOPROPANOL/WATER/NaCl MIXTURES

Table A1. Experimentally measured liquid-liquid (LL), liquid-solid (LS) and liquid-liquid-solid (LLS) phase boundaries at room temperature and atmospheric pressure. The NaCl and isopropanol contents are reported in mass fractions.

Temperature, ˚C	Boundary	NaCl Content, wt	Isopropanol Content, wt
21	LL	0.141	0.184
21	LL	0.052	0.540
21	LL	0.082	0.390
21	LL	0.097	0.333
21	LL	0.159	0.158
21	LL	0.044	0.582
21	LL	0.058	0.507
21	LL	0.089	0.379
21	LL	0.105	0.312
21	LL	0.029	0.666
21	LL	0.167	0.141
21	LL	0.157	0.152
21	LL	0.124	0.230
21	LL	0.071	0.437
21	LL	0.032	0.639
21	LL	0.217	0.083
21	LL	0.125	0.239
21	LL	0.073	0.435
21	LS	0.239	0.034
21	LS	0.233	0.048
21	LS	0.014	0.751
21	LS	0.014	0.772
21	LS	0.265	0.000
21	LLS	0.187	0.186
21	LLS	0.049	0.649
21	LLS	0.067	0.586
21	LLS	0.107	0.456
21	LLS	0.126	0.375
21	LLS	0.194	0.164
21	LLS	0.184	0.178
21	LLS	0.156	0.289
21	LLS	0.086	0.529
21	LLS	0.035	0.693
21	LLS	0.217	0.083
21	LLS	0.156	0.300
21	LLS	0.087	0.518

Table A2. Experimentally measured liquid-liquid (LL), liquid-solid (LS) and liquid-liquid-solid (LLS) phase boundaries at 50°C and atmospheric pressure. The NaCl and isopropanol contents are reported in mass fractions.

Temperature, ˚C	Boundary	NaCl Content, wt	Isopropanol Content, wt
50.0	LL	0.042	0.564
49.5	LL	0.080	0.347
49.2	LL	0.081	0.353
50.0	LL	0.111	0.232
48.3	LL	0.153	0.146
49.2	LL	0.182	0.104
50.0	LL	0.122	0.191
50.0	LL	0.097	0.277
50.1	LL	0.075	0.376
50.0	LL	0.062	0.440
49.7	LL	0.147	0.141
50.1	LL	0.111	0.226
50.1	LL	0.028	0.652
50.1	LL	0.045	0.527
49.4	LS	0.236	0.068
50.1	LS	0.014	0.812
50.0	LS	0.269	0.000
50.0	LS	0.260	0.020
49.5	LLS	0.108	0.473
49.2	LLS	0.106	0.461
51.4	LLS	0.157	0.326
52.2	LLS	0.193	0.183
50.0	LLS	0.214	0.122
50.0	LLS	0.170	0.266
50.0	LLS	0.136	0.386
50.0	LLS	0.098	0.489
49.5	LLS	0.079	0.563
50.0	LLS	0.195	0.187
50.1	LLS	0.156	0.318
49.9	LLS	0.032	0.732
50.1	LLS	0.055	0.651
50.0	LLS	0.050	0.678

Table A3. Experimentally measured liquid-liquid (LL), liquid-solid (LS) and liquid-liquid-solid (LLS) phase boundaries at 70°C and atmospheric pressure. The NaCl and isopropanol contents are reported in mass fractions.

Temperature, ˚C	Boundary	NaCl Content, wt	Isopropanol Content, wt
70.1	LL	0.119	0.205
70.1	LL	0.159	0.131
70.1	LL	0.096	0.267
70.1	LL	0.080	0.329
70.1	LL	0.065	0.416
69.9	LL	0.052	0.479
69.9	LL	0.025	0.646
69.9	LL	0.195	0.093
69.9	LL	0.017	0.725
70.0	LS	0.243	0.054
70.0	LS	0.252	0.033
70.0	LS	0.273	0.000
69.9	LS	0.010	0.840
70.0	LLS	0.171	0.293
70.0	LLS	0.208	0.172
70.0	LLS	0.138	0.385
70.0	LLS	0.112	0.462
70.1	LLS	0.086	0.551
70.0	LLS	0.067	0.621
70.0	LLS	0.029	0.745
70.0	LLS	0.228	0.108
70.0	LLS	0.019	0.774

APPENDIX B:

EXPERIMENTALLY MEASURED LIQUID-LIQUID PHASE COMPOSITIONS AND CALCULATED PLAIT POINTS

Table B1. Measured aqueous and organic phase compositions at atmospheric pressure. The NaCl, isopropanol and water content in the phases is reported as mass fraction.

Aqueous Phase			Organic Phase		
NaCl, wt	**Isopropanol, wt**	**Water, wt**	**NaCl, wt**	**Isopropanol, wt**	**Water, wt**
0°C					
0.138	0.272	0.590	0.048	0.579	0.373
0.167	0.201	0.632	0.031	0.643	0.325
0.181	0.170	0.649	0.030	0.680	0.290
21°C					
0.159	0.155	0.685	0.028	0.633	0.339
0.128	0.226	0.645	0.042	0.538	0.420
0.124	0.240	0.635	0.044	0.525	0.430
0.187	0.102	0.711	0.022	0.688	0.290
0.201	0.085	0.714	0.018	0.707	0.274
50°C					
0.151	0.129	0.720	0.023	0.648	0.330
0.169	0.103	0.727	0.018	0.684	0.298
0.125	0.191	0.684	0.030	0.571	0.400
0.137	0.160	0.702	0.027	0.610	0.363
70°C					
0.156	0.120	0.724	0.020	0.663	0.317
0.123	0.188	0.689	0.032	0.571	0.397
0.136	0.155	0.709	0.027	0.633	0.340

Table B2. Calculated plait points at atmospheric pressure. The NaCl, isopropanol and water content are reported as mass fraction.

Temperature, ˚C	NaCl, wt	Isopropanol, wt	Water, wt
21	0.078	0.401	0.521
50	0.064	0.423	0.513
70	0.069	0.382	0.549

APPENDIX C:

EXPERIMENTALLY MEASURED LIQUID-VAPOR TEMPERATURES AND PHASE COMPOSITIONS.

Table C1. Measured normal boiling points of mixtures NaCl and water. The reported compositions, in mass fraction, are those in the liquid phase.

Temperature, ˚C	NaCl, wt	Water, wt
99.5	0	1
100.4	0.058	0.942
100.8	0.081	0.919
101.3	0.105	0.895
101.6	0.117	0.883
101.9	0.134	0.866
102.6	0.149	0.851
105.4	0.223	0.777

Table C2. Measured normal boiling points and liquid-vapor phase compositions of isopropanol/water mixtures. The isopropanol and water content are reported as mass fraction.

Temperature, ˚C	Vapor Phase		Liquid Phase	
	Isopropanol, wt	Water, wt	Isopropanol, wt	Water, wt
79.7	0.848	0.151	0.796	0.203
80.1	0.844	0.155	0.737	0.262
80.2	0.894	0.105	0.894	0.105
81.2	0.819	0.180	0.603	0.396
81.8	0.798	0.201	0.480	0.519
87.7	0.699	0.300	0.118	0.881
89.3	0.662	0.338	0.091	0.908
89.6	0.608	0.391	0.075	0.924
90.6	0.584	0.415	0.067	0.932
91.1	0.612	0.387	0.069	0.930
92.0	0.602	0.397	0.043	0.956
93.7	0.531	0.468	0.042	0.957
93.7	0.512	0.487	0.045	0.954
94.6	0.478	0.522	0.038	0.961
95.5	0.321	0.678	0.035	0.964
95.8	0.391	0.608	0.018	0.981
97.0	0.234	0.765	0.018	0.981

Table C3. Measured normal boiling points and liquid-vapor phase compositions of isopropanol/water/NaCl mixtures. The isopropanol, water and NaCl contents are reported as mass fractions.

Temperature, °C	Liquid Phase			Vapor Phase	
	NaCl, wt	Isopropanol, wt	Water, wt	Isopropanol, wt	Water, wt
94.1	0.006	0.029	0.964	0.476	0.524
80.3	0.011	0.659	0.331	0.859	0.141
98.0	0.021	0.014	0.965	0.212	0.788
80.9	0.028	0.379	0.593	0.843	0.157
90.0	0.046	0.041	0.912	0.547	0.453
83.8	0.048	0.133	0.819	0.774	0.226
80.9	0.049	0.441	0.510	0.856	0.144
81.5	0.049	0.340	0.611	0.834	0.166
80.3	0.064	0.362	0.575	0.844	0.156
97.6	0.072	0.013	0.915	0.158	0.842
84.6	0.100	0.079	0.821	0.758	0.242
81.2	0.101	0.193	0.706	0.818	0.182
95.7	0.102	0.019	0.879	0.498	0.502
80.8	0.116	0.194	0.690	0.825	0.175
87.7	0.208	0.023	0.769	0.794	0.206